Simulation of the hydrological impacts of climate change on a restored floodplain

Julian R. Thompson, Honeyeh Iravani, Hannah M. Clilverd, Carl D. Sayer, Catherine M. Heppell & Jan C. Axmacher

Accepted author version posted online: 17 Oct 2017.
Published online: 06 Nov 2017.

Submit your article to this journal ☑

Article views: 132

View related articles ☑

View Crossmark data ☑

Citing articles: 1 View citing articles ☑

IAHS AISH

Taylor & Francis
Taylor & Francis Group

OPEN ACCESS

Check for updates

Simulation of the hydrological impacts of climate change on a restored floodplain

Julian R. Thompson[a], Honeyeh Iravani[a], Hannah M. Clilverd[a,b], Carl D. Sayer[a], Catherine M. Heppell[c] and Jan C. Axmacher[a]

[a]UCL Department of Geography, University College London, London, UK; [b]Department of Natural Resources and Environmental Management, University of Hawai'i, Mānoa, Honolulu, Hawai'i, USA; [c]School of Geography, Queen Mary University of London, London, UK

ABSTRACT

Thirty UK Climate Projections 2009 (UKCP09) scenarios are simulated using a MIKE SHE/MIKE 11 model of a restored floodplain in eastern England. Annual precipitation exhibits uncertainty in direction of change. Extreme changes (10 and 90% probability) range between −27 and +30%. The central probability projects small declines (<−4%). Wetter winters and drier summers predominate. Potential evapotranspiration increases for most scenarios (annual range of change: −41 to +2%). Declines in mean discharge predominate (range: −41 to +25%). Reductions of 11–17% are projected for the central probability. High and low flows, and the frequency of bankfull discharge exceedence reduce in most cases. Duration of winter high floodplain water tables declines. Summer water tables are on average at least 0.11 and 0.18 m lower for the 2050s and 2080s, respectively. Flood extent declines in most scenarios. Drier conditions will likely induce ecological responses including impacts on floodplain vegetation.

Introduction

Flooding and associated delivery of sediment and nutrients exert important controls on natural floodplains. The diversity of hydro-ecological conditions that result from disturbances due to regular floods and high water tables drives high habitat heterogeneity and primary productivity (Grevilliot *et al.* 1998, Ward 1998, Gowing *et al.* 2002, Woodcock *et al.* 2005). The diverse array of microhabitats commonly found on natural floodplains is a key driver of their high biodiversity (Junk *et al.* 1989, Silvertown *et al.* 1999, Ward *et al.* 1999, Tockner and Stanford 2002, Dwire *et al.* 2006, Freeman *et al.* 2007, Arthington *et al.* 2015). Similarly, strong hydrological links underpin numerous ecosystem services provided by rivers and their floodplains (Zedler and Kercher 2005, Kondolf *et al.* 2006). These services include provision of habitat and maintenance of biodiversity that in turn support catchment-wide fisheries as well as nutrient retention, floodwater storage and flood peak attenuation (Hill 1996, Ward *et al.* 2002, Bullock and Acreman 2003, Baker and Vervier 2004, Forshay and Stanley 2005, Acreman *et al.* 2007, Naiman *et al.* 2010).

However, many rivers around the world have been embanked, channelized and deepened to improve agricultural productivity on floodplains and to protect land from flooding (Buijse *et al.* 2002, Tockner and Stanford 2002). For example, 40% of total river length in England and Wales has been classified as severely modified (Environment Agency 2010). Channelization and embanking restricts or even completely disables overbank flow mechanisms. This reduces the magnitude and frequency of transfers of water, sediment and nutrients between rivers and their floodplains (e.g. Tockner *et al.* 1999, Wyżga 2001, Antheunisse *et al.* 2006). Resulting changes in floodplain hydrological conditions contribute to significant ecological degradation, with consequent impacts on ecosystem service delivery (Erskine 1992, Ward and Stanford 1995, Petts and Calow 1996, Nilsson and Svedmark 2002, Pedroli *et al.* 2002).

Re-establishing hydrological connections between rivers and floodplains is an increasingly common management approach to restoring these aquatic ecosystems (e.g. Acreman *et al.* 2003, Blackwell and Maltby 2006, Pescott and Wentworth 2011, Addy *et al.* 2016). Floodplain restoration, frequently involving reconfiguration of river channels and removal of embankments, is often designed with a number of objectives. A more natural, dynamic, flood-pulsed hydrological regime benefits floodplain biodiversity and ecosystem

services such as nutrient retention, whilst temporary storage of floodwater contributes to catchment-wide flood management strategies (Muhar *et al.* 1995, Acreman *et al.* 2003, Bernhardt *et al.* 2005, Blackwell and Maltby 2006, Pescott and Wentworth 2011).

Assessment of the impacts of restoration upon floodplain hydrology, and in turn inferring likely ecological responses, ideally requires long-term monitoring both before and after restoration (Addy *et al.* 2016). However, such monitoring programmes are rare (Kondolf 1995, Darby and Sear 2008). Extended monitoring before restoration is often impractical given financial and other pressures to proceed with restoration as soon as possible within project lifespans. Similarly, funding for extensive post-restoration monitoring is only infrequently available. Even when monitoring is undertaken before and after restoration, relatively short records and inter-annual climate variability complicate direct comparison of pre- and post-restoration conditions (e.g. Clilverd *et al.* 2013). Added uncertainty over future hydrological conditions on restored floodplains is linked to climate change. Unequivocal climate warming (IPCC 2014) will alter precipitation and evapotranspiration, which will, in turn, impact river flows and groundwater levels (e.g. Kundzewicz *et al.* 2007, Bates *et al.* 2008). Irrespective of floodplain restoration, changes in climate and resultant modifications to local and catchment-wide hydrological responses are likely to impact hydrological conditions within floodplains and other wetlands (e.g. Acreman *et al.* 2009, Erwin 2009, Thompson *et al.* 2009). These impacts on restored river–floodplain systems remain largely unknown.

Hydrological/hydraulic modelling has huge potential to tackle these issues. Models can enhance understanding of the hydrological functioning of floodplains and similar wetlands, which can, in turn, inform improvements in their management (e.g. Thompson *et al.* 2004, House *et al.* 2016b). Modelling provides a means of assessing potential impacts of river and floodplain restoration (e.g. Thompson 2004, Hammersmark *et al.* 2008, Clilverd *et al.* 2016), as well as investigating the consequences of climate change (e.g. Thompson *et al.* 2009, Karim *et al.* 2016, House *et al.* 2016a, 2017). The current study employs a coupled hydrological/hydraulic model that was originally designed to assess the hydrological impacts of restoring a small floodplain in eastern England (Clilverd *et al.* 2016). The impacts of climate change upon the hydrological conditions (river flow, groundwater level, and flood extent and frequency) within the post-restoration floodplain are investigated by forcing model inputs with projections of future UK climate.

Methods

Study site: Hunworth Meadow

Hunworth Meadow is located adjacent to the River Glaven, a small (length: 17 km, catchment area: 115 km^2), lowland, calcareous river in North Norfolk, UK (Fig. 1). The catchment has a chalk bedrock overlain by chalk-rich sandy till and glaciogenic sand and gravel (Moorlock *et al.* 2002). Floodplain soils consist of alluvial deposits up to 2 m thick (Clilverd *et al.* 2013). Catchment land cover is a mosaic of agricultural land, deciduous and coniferous woodland and grazing meadows. Regional mean annual rainfall (1985–2015) is approximately 620 mm, exceeding annual evapotranspiration of about 600 mm. Rainfall is higher in autumn and winter, whilst in summer potential evapotranspiration commonly exceeds precipitation. River flow is typical of the region's chalk streams, with highest flows occurring in winter, whilst the mean baseflow index for the gauging station at Hunworth, immediately upstream of the meadow, is 0.81 (Clilverd *et al.* 2013). Mean discharge at this station for the period 2001–2010 is 0.26 m^3 s^{-1} with the largest recorded discharge being 3.1 m^3 s^{-1} (Clilverd *et al.* 2016). Many reaches of the River Glaven have been modified through channel deepening and straightening and, although conservation work has removed embankments along some reaches, along much of its length embankments disconnect the river from its floodplain. Some floodplains have also been subject to extensive drainage and the conversion for agricultural use (Clilverd *et al.* 2013).

Hunworth Meadow, which before restoration was typical of many floodplains along the Glaven, is located in the middle reaches of the river. It is approximately 400 m long, 40–80 m wide and has an area approaching 3 ha. Topography follows a general downstream gradient, with a fall of less than 1.0 m over the length of the meadow. The meadow is bounded to the northeast by an arable and woodland hillslope, whilst the river lies to the southwest (Fig. 1). Prior to restoration, this river section was constrained by embankments. These ranged in height from 0.4 to 1.1 m above the meadow surface and were designed to limit overbank flows from the river onto the floodplain (Clilverd *et al.* 2013). Mean channel width and depth (from the top of the embankment to the deepest point of the channel) were 3.7 and 1.4 m, respectively. Whilst there is an agricultural ditch running parallel to the river and close to the foot of the hillslope, during the study it was blocked at its downstream end, resulting in near-permanent water within a shallow pond at the lowest part of the floodplain. The meadow's vegetation before
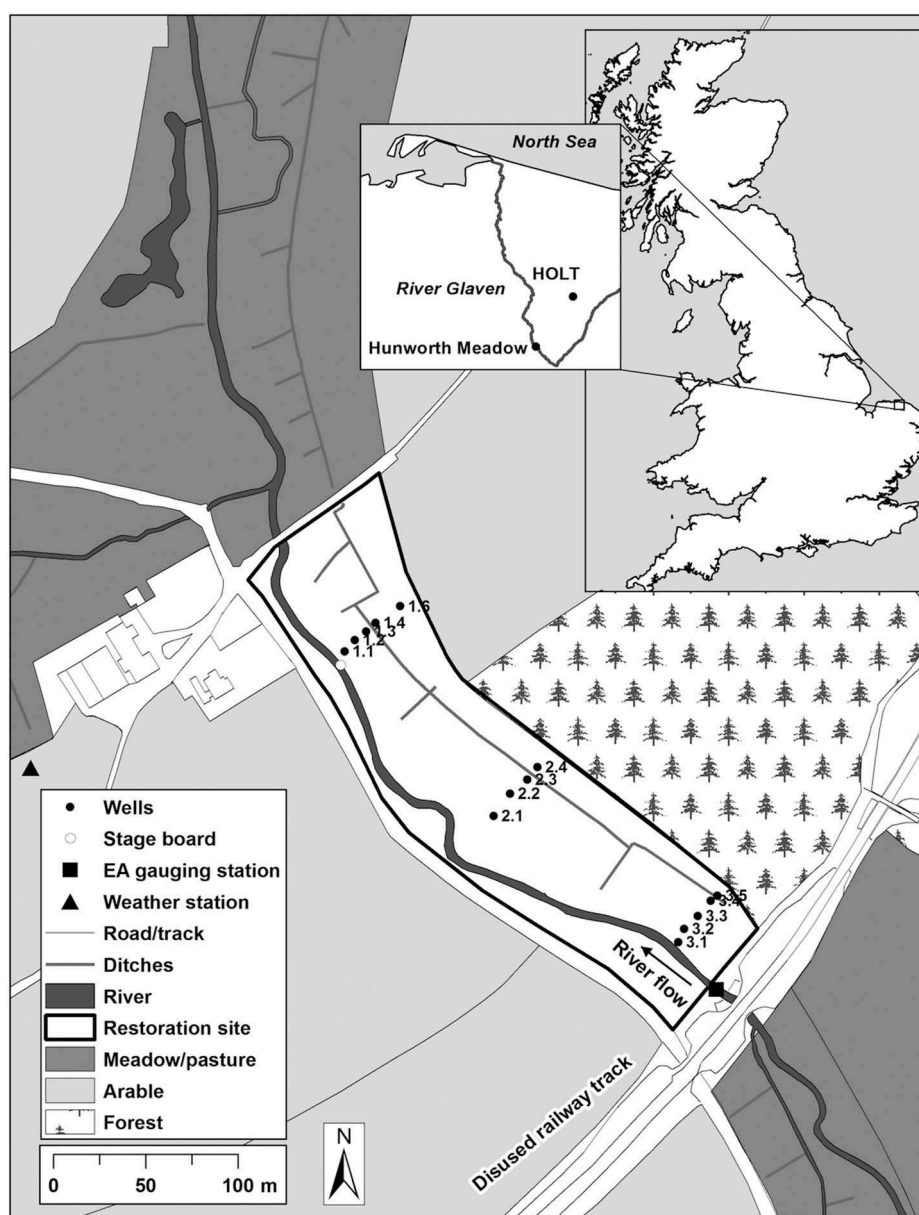
Figure 1. The Hunworth Meadow restoration site, north Norfolk. The locations of shallow groundwater monitoring wells and the automatic weather station are indicated.

restoration comprised a degraded *Holcus lanatus–Juncus effusus* rush pasture community (MG10 according to the UK National Vegetation Classification, NVC, Rodwell 1992), typically associated with waterlogged soils (Clilverd 2016).

Restoration works were undertaken at Hunworth Meadow in March 2009. With the exception of a short (approx. 20 m) section left to protect European water vole (*Arvicola amphibious*) burrows, the embankments were removed along the length of the river. As a result, the elevation of the riverbanks was lowered to the level of the adjacent meadow, whilst channel depth and cross-sectional area were reduced by approximately 44 and 60%, respectively (Clilverd

et al. 2013, 2016). The rationale for the restoration was to improve the connection between the river and its floodplain, improve flood storage and establish a floodplain hydrological regime that would diversify wet meadow vegetation (e.g. Hammersmark *et al.* 2008, Castellarin *et al.* 2010, Viers *et al.* 2012).

Hunworth Meadow coupled hydrological/hydraulic modelling

Clilverd *et al.* (2016) developed models of pre-restoration (embanked) and post-restoration (no embankment) conditions using the MIKE SHE/MIKE 11 modelling system, which has proven utility for floodplain and wetland

environments (e.g. Thompson 2004, Thompson et al. 2004, Hammersmark et al. 2008, Duranel et al. 2016, House et al. 2016b). Since Clilverd et al. (2016) provide a detailed description of the Hunworth models, only a brief account is provided herein.

Pre- and post-restoration models only differed in the representation of floodplain topography in the location of the embankments and cross-sections of the River Glaven. Topographic data were derived from dGPS surveys conducted before and after embankment removal (Clilverd et al. 2013). These data were resampled to the 5038 cells of the 5 m × 5 m model grid. The model domain included Hunworth Meadow and extended to the summits of the hillsides on either side of the river. Upstream and downstream limits of the domain coincided with a disused railway embankment and a smaller embankment carrying an agricultural track, respectively. Given the small size of the model domain, spatially uniform precipitation and potential evapotranspiration (PET) were specified. Daily precipitation data were initially provided by an automatic weather station (AWS) installed 100 m from the meadow (Fig. 1) supplemented by a nearby (<10 km) UK Met Office meteorological station at Mannington Hall. Daily Penman-Monteith PET (Monteith 1965) was calculated from air temperature, net radiation, relative humidity and wind speed from the AWS (Clilverd et al. 2013).

A relatively simple one-layer saturated zone was employed using the 3D finite difference scheme to represent average hydrogeological conditions in the upper alluvial and glacial soils, which are separated from the underlying chalk by low permeability boulder clay. Hydraulic conductivity was adjusted during calibration, with initial values guided by piezometer slug tests (Clilverd et al. 2013). An area of much lower hydraulic conductivity was specified in the location of the pond at the downstream end of the meadow. Zero flow boundaries were applied along the summits of the hillsides and the upstream end of the meadow, based on assumptions that the groundwater divide follows the topographic divide and foundations of the railway embankment restrict subsurface flow. In contrast, and to facilitate potential subsurface flow perpendicular to the river, a constant head was specified across the downstream boundary of the meadow using mean groundwater elevation from a well transect (see below) towards the downstream end of the meadow. Relatively small-scale, rapid runoff along the base of the hillside and along the agricultural ditch was represented using the saturated zone drainage option with drainage levels and time constants being varied during calibration. The conceptual two-layer water balance

unsaturated zone scheme was used. This is particularly appropriate in high water table situations such as those within the meadow (e.g. Thompson 2012). A uniform soil was specified across the model domain, with each of the five unsaturated zone parameters (infiltration rate, soil water content at saturation, field capacity and wilting point, and the ET depth) being varied during calibration but guided by slug tests, water release characteristics derived from sandbox experiments, soil porosity and the literature (Chubarova 1972, Das 2002, DHI 2007, Zotarelli et al. 2010).

Four land-use classes were defined within the MIKE SHE models: riparian grassland, mixed deciduous/coniferous woodland, arable land and roads/buildings. Root depths and leaf area index (LAI) for each of the vegetation classes were specified from the literature (Canadell et al. 1996, Hough and Jones 1997, Herbst et al. 2008, Thorup-Kristensen et al. 2009, FAO 2013) and included temporal variations to reflect seasonal vegetation development. Root depth and LAI were both defined as 0 for roads/buildings. The same landcover classes were used to distribute the Manning's roughness for overland flow, which was varied during calibration but guided by literature values (USDA 1986, Thompson 2004).

Two MIKE 11 models were developed, one for the original embanked conditions and the other for postembankment removal. Each model was dynamically coupled to the corresponding (embanked/restored) MIKE SHE model using the approach described by Thompson et al. (2004) and DHI (2007). The reach of the River Glaven running immediately upstream, through and downstream of the meadow was digitized from 1:10 000 Ordnance Survey digital data (LandLine.Plus). Cross-sections were specified at approximately 10-m intervals using results from the pre- and post-restoration dGPS surveys. Daily mean discharge from the gauging station immediately above the meadow was specified as the upstream boundary condition, whilst a constant water level just above the riverbed was applied to the lower boundary. This prevented the river drying out and enabled discharge from the downstream end of MIKE 11, whilst the extension of the river model below the meadow avoided the specified boundary condition from impacting simulated water levels within the study reach (e.g. Thompson et al. 2004). A time-varying Manning's n roughness coefficient was specified throughout the MIKE 11 model using the method adopted by House et al. (2016b). This represented seasonal macrophyte growth and dieback, which has been shown to impact water levels within the Glaven (Clilverd et al. 2013). Manning's n values and the macrophyte growth cycle were guided

by the literature (Flynn et al. 2002, House et al. 2016b). In the absence of information on the spatial distribution of macrophytes and in common with House et al. (2016b), this time-varying Manning's n value was spatially uniform along the length of the MIKE 11 model. The MIKE SHE/MIKE 11 coupling included the specification of flood codes to determine the MIKE SHE grid squares that could be directly inundated from MIKE 11. These cells comprised the immediate riparian area including those coincident with the MIKE 11 model, those containing the embankments (if present) and a zone up to 10 m (i.e. two MIKE SHE grid cells) onto the meadow. These cells would flood if MIKE 11 simulated water levels exceeded their elevation. Once a cell was flooded, the overland flow component of MIKE SHE would simulate surface water movement onto adjacent grid cells further from the river (see Thompson et al. 2004).

The maximum model time step was 24 h for most MIKE SHE components, the exception being the finite difference overland flow component, where a 0.25-h time step was required for numerical stability. MIKE 11 models were set up to run at 1-min time steps. Model results were stored at a 24-h interval to coincide with observations used in model calibration and validation. These observations were primarily from 10 shallow (1–2 m deep) wells installed in three transects (Fig. 1). Mean daily groundwater levels were obtained from pressure transducers installed in the wells and were supplemented by less frequent manual well dipping (see Clilverd et al. 2013). A three-stage calibration/validation approach was employed. Initially the pre-restoration model was calibrated using the 13 months between 22 February 2007 and 14 March 2008 followed by validation using the subsequent 12-month period (15 March 2008–15 March 2009), the end of which coincided with embankment removal. A second validation was undertaken by specifying calibrated parameter values within the post-restoration model, which was run for the 16 months after embankment removal (29 March 2009–25 July 2010). Calibration was initially undertaken using an automatic procedure (e.g. Madsen 2000, 2003) using a coarser 15 m × 15 m model grid to reduce computational time. Final parameter values were refined manually using the 5 m × 5 m model with performance assessed using the root mean square error (RMSE), the Pearson correlation coefficient (r), and the Nash-Sutcliffe efficiency coefficient (NSE; Nash and Sutcliffe 1970). These statistics were also used in assessing model performance for the validation periods.

Clilverd et al. (2016) discussed the model results in detail, demonstrating generally very good agreement between observed and simulated groundwater levels throughout the calibration and validation periods. The mean error was typically less than ±0.05 m, whilst the correlation coefficient (r) averaged 0.85, 0.80 and 0.85 for the calibration and pre- and post-restoration validation periods, respectively. NSE values were between 0.50 and 0.80 for most wells, suggesting fair to good performance. The observed rapid responses in groundwater levels during high magnitude rainfall events, especially close to the river, and the more gradual declines through spring and summer were both clearly reproduced (e.g. Fig. 2). Simulated seasonal fluctuations in levels in the range of 0.40–0.60 cm were also close to those observed on the meadow. Given the good performance of the models for both pre- and post-restoration conditions, Clilverd et al. (2016) assessed the impacts of embankment removal by running each model over an extended period (2001–2010) which encompassed a range of climate and river flow conditions. As for the calibration and validation periods, the Hunworth gauging station provided upstream boundary conditions for MIKE 11. In the absence of data from the automatic weather station, precipitation and Penman-Monteith PET for the MIKE SHE models were derived from the Mannington Hall meteorological station. Results demonstrated that the largest impacts of embankment removal were the increase in widespread inundation at high river flows and much more frequent localized flooding during smaller events. Enhanced river–floodplain hydrological connectivity led to some raised groundwater levels, in particular close to the river, and increased subsurface storage. It was argued that a more natural wetland ecotone would eventually form following the restoration, in which frequent localized flooding would be a dominant factor. Assessing whether such changes will persist under future climatic conditions provides the impetus for the current study.

Climate change scenarios

Climate change scenarios were developed using the change/delta factor approach. Whilst this method assumes that climate variability does not change, and as such it does not represent changes in event frequency and distribution (Chiew et al. 1995, Graham et al. 2007), it does permit a robust comparison of average outcomes and as result it has been extensively used in hydrological studies of climate change (e.g. Arnell and Reynard 1996, Arnell 2004, Thompson et al. 2009, 2016, Ho et al. 2016). Baseline precipitation and PET data employed within the MIKE SHE/MIKE 11 model of Hunworth Meadow were perturbed using
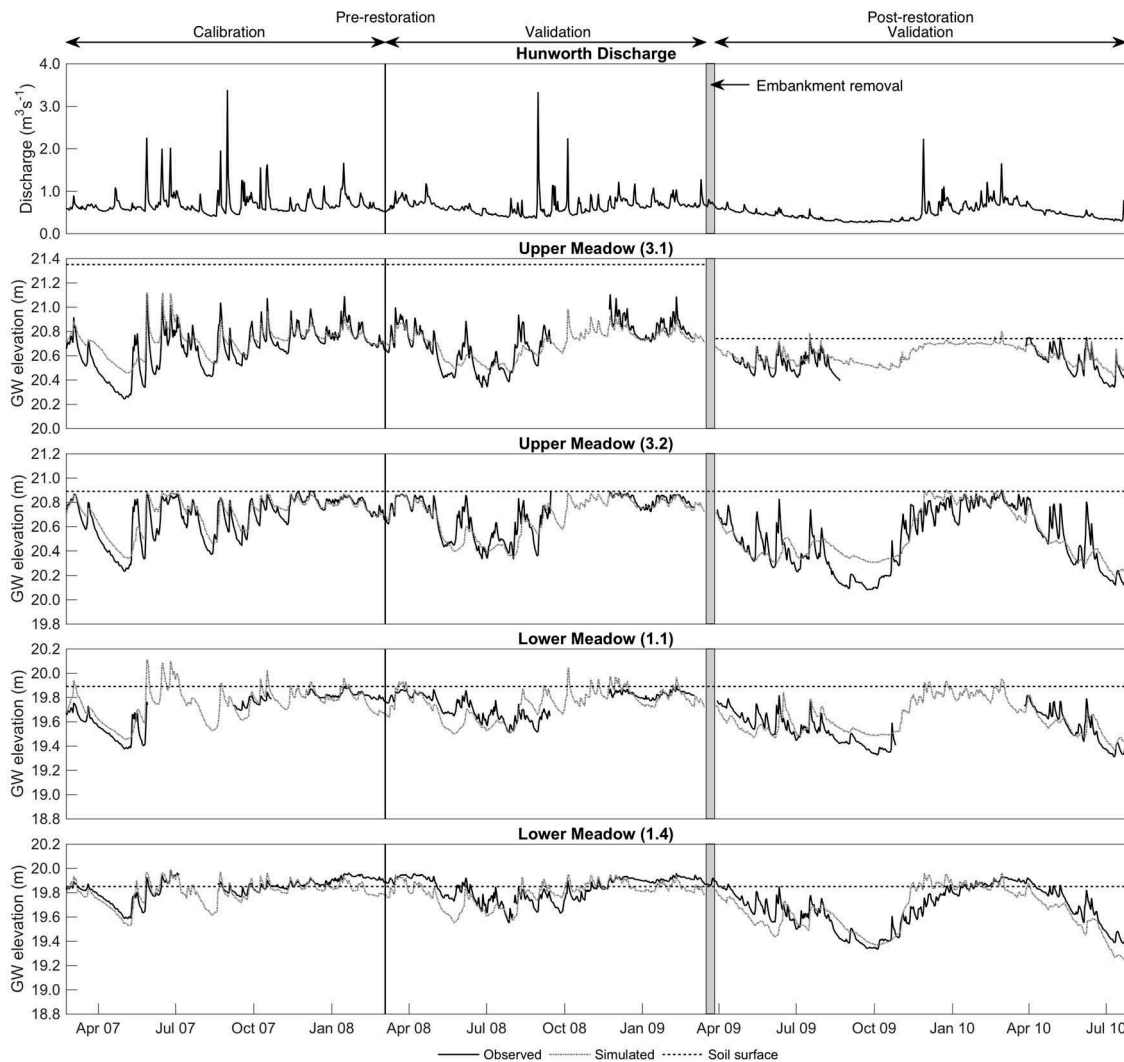
Figure 2. Observed and simulated groundwater depths and corresponding river flow at the Hunworth gauging station for the calibration and validation periods for four representative wells across Hunworth Meadow. The date of embankment removal in March 2009 is indicated. The locations of the wells are indicated in Figure 1.

the 2009 UK Climate Projections (UKCP09) following the method described by Thompson (2012). UKCP09, described in detail by Jenkins *et al.* (2009), provides probabilistic projections for a series of atmospheric variables under three emission scenarios; Low, Medium and High, corresponding to the B1, A1B and A1FI scenarios in the IPCC Special Report on Emissions Scenarios (SRES, IPCC 2000). Probability distribution functions are provided for each atmospheric variable that are designed to represent uncertainty in future climate. Projections are based on a large perturbed physics ensemble using the Met Office Hadley Centre's HadCM3 global climate model and results from a further 12 global climate models (GCMs). GCM projections are downscaled to a 25 × 25 km grid using the HadRM3 regional climate model (Murphy *et al.* 2009) and are available for seven

overlapping 30-year time slices that step forward by a decade from 2010–2039 to 2070–2099. Changes in atmospheric variables with reference to a 30-year baseline period (1961–1990) are available for monthly, seasonal and annual average periods.

Projections for the three emission scenarios for the 2040–2069 and 2070–2099 time slices (referred to as the 2050s and 2080s, respectively) were selected to represent conditions towards the middle and end of the current century. However, since the baseline simulation period for the Hunworth model (2001–2010) falls outside the UKCP09 baseline period, results are likely to be representative of conditions towards the latter part and immediately beyond the end of each time slice (see Thompson *et al.* 2009). Monthly changes in precipitation, minimum, mean and maximum temperatures (°C), relative humidity (%) and total

downward surface shortwave flux (W m^2) were abstracted from the HadRM3 model grid in which the Hunworth Meadow is located. This was undertaken for probabilities between the 10 and 90% levels in 20% increments, giving a total of 30 scenarios (15 for each time slice). In accordance with the recommendations of Murphy *et al.* (2009), extreme probabilities beyond this range were not used. This range of probabilities includes the central estimate of change (the change that is as likely as not to be exceeded, i.e. the 50% probability level) and is bounded by the changes that are very likely to be exceeded (10% probability level) and those that are very unlikely to be exceeded (90% probability level). Scenarios are referred to in the form 2050M$_{50}$ (i.e. the 2050 time slice, Medium emission scenario, 50% probability level). The original daily precipitation data for the period 2001–2010 were multiplied by the UKCP09 monthly percentage changes to provide scenario precipitation time series (Thompson 2012). In the same way, projected changes in minimum, mean and maximum temperatures, relative humidity and total downward surface shortwave flux were used to perturb the corresponding meteorological time series. In the absence of scenario wind speed within the UKCP09 projections, the original time series was retained. Subsequently, perturbed meteorological data were used to recalculate Penman-Monteith PET for each scenario (e.g. Thompson *et al.* 2009, 2014).

Development of scenario discharge was based on the approach adopted by House *et al.* (2016a). A rainfall–runoff model of the 37.6 km^2 catchment above the Hunworth gauging station was developed using MIKE NAM. This is a deterministic, lumped conceptual catchment model with continuous accounting of soil moisture within interrelated storages (surface, soil and groundwater) and the flows between them (e.g. DHI 2009, Hafezparast *et al.* 2013). The simulation period for the NAM model was identical to that employed in the assessment of the impacts of embankment removal using the MIKE SHE/MIKE 11 model of Hunworth Meadow (i.e. 2001–2010). Daily precipitation and PET for the NAM model were specified as the same time series employed in the MIKE SHE/MIKE 11 model. Spatially uniform precipitation and PET were considered appropriate given the relatively small size of the catchment. Calibration was based on comparisons between observed and simulated discharges at the Hunworth gauging station, with the relatively short duration of the record for this station limiting the traditional split sample approach. Initially an automatic multiple objective calibration routine was employed with the objective functions based on daily discharge comprising the overall water balance and RMSE and

the RMSE error for both high and low flows. The parameters in the automatic calibration included maximum water content in the surface and root zone storage, the overland flow runoff coefficient, time constants for interflow, routing overland flow and routing baseflow, and the root zone threshold values for overland flow, interflow and groundwater recharge. Parameter values defined at the end of the automatic calibration were subsequently fine-tuned manually (e.g. Thompson *et al.* 2013), with model performance being evaluated for both daily and monthly mean discharge using NSE, *r* and bias (Dv, i.e. the percentage deviation in simulated mean flow from the observed mean flow; Henriksen *et al.* 2003). Monthly climate change delta factors for discharge were established by running the NAM model with the perturbed precipitation and PET for each scenario. Differences between baseline and scenario mean monthly discharges, expressed as a percentage, were subsequently applied to the original discharge record for Hunworth.

The MIKE SHE/MIKE 11 model of post-restoration conditions was used to simulate each scenario by substituting the original precipitation and PET time series within MIKE SHE with those established using the methods described above. Perturbed river discharge time series was specified at the upstream boundary for the coupled MIKE 11 model. The same 2001–2010 period was employed for each scenario, with results being compared to those from the baseline model (i.e. the model using the original precipitation, PET and discharge time series).

Results

Scenario climate

Mean annual total precipitation and PET for the 2001–2010 baseline and each climate change scenario are shown in the top half of Table 1. Figure 3 shows the mean monthly distribution of precipitation and PET for the baseline and each scenario. Changes in precipitation due to different probability levels vary not only in magnitude but also in direction. Mean annual precipitation declines for probability levels between 10 and 50% and increases for higher probability levels (70 and 90%). Changes in annual precipitation (baseline: 773.2 mm) that are as likely as not to be exceeded (50% probability level) are associated with very small reductions. For the 2050s these are between 13.9 mm (1.8%, Low) and 21.2 mm (2.7%, Medium). Reductions are similarly small for the 2080s, ranging between 9.9 mm (1.3%, Low) and 27.1 mm (3.5%, High). Declines in mean annual precipitation for the 2050s

Table 1. Mean annual precipitation, potential evapotranspiration (PET) and net precipitation (precipitation – PET) (mm), and number (% of the total 120 months in brackets) when precipitation > PET (i.e. net precipitation is positive) for the baseline and each UKCP09 scenario. Shaded cells indicate reductions compared to the baseline.

		10%	30%	50%	70%	90%
Mean annual precipitation: Baseline 773.2						
2050s	L	609.0	696.6	759.3	828.4	943.7
	M	608.1	689.8	752.0	820.1	933.1
	H	601.9	690.8	758.6	833.4	958.2
2080s	L	609.5	697.0	763.3	836.1	957.1
	M	585.4	678.4	750.0	829.5	963.7
	H	563.0	664.8	746.1	839.3	1003.6
Mean annual PET: Baseline 509.0						
2050s	L	499.6	537.1	564.4	593.0	637.9
	M	500.1	538.1	565.6	594.9	641.5
	H	502.7	543.5	573.2	605.2	656.9
2080s	L	501.9	542.8	572.7	604.9	656.6
	M	504.3	549.7	583.2	620.1	681.0
	H	507.2	560.9	601.3	645.8	719.1
Mean annual net precipitation: Baseline 264.2						
2050s	L	109.5	159.5	194.9	235.5	305.8
	M	108.0	151.8	186.4	225.2	291.5
	H	99.2	147.2	185.4	228.2	301.3
2080s	L	107.6	154.2	190.6	231.2	300.5
	M	81.2	128.7	166.8	209.5	282.7
	H	55.8	103.9	144.8	193.4	284.5
Months where precipitation > PET: Baseline 76 (63%)						
2050s	L	66 (55%)	69 (58%)	71 (59%)	74 (62%)	75 (63%)
	M	63 (53%)	66 (55%)	69 (58%)	72 (60%)	74 (62%)
	H	65 (54%)	66 (55%)	68 (57%)	72 (60%)	74 (62%)
2080s	L	65 (54%)	68 (57%)	69 (58%)	71 (59%)	75 (63%)
	M	62 (52%)	65 (54%)	66 (55%)	68 (57%)	72 (60%)
	H	62 (52%)	65 (54%)	63 (53%)	66 (55%)	70 (58%)

that are very likely to be exceeded (10% probability) vary between 164.2 mm (21.2%, Low) and 171.3 mm (22.2%, High). The corresponding figures for the 2080s indicate maximum projected declines of between 163.7 mm (21.2%) and 210.2 mm (27.2%), respectively. At the other extreme, increases in annual precipitation that are very unlikely to be exceeded (90% probability) are of similar magnitude to declines projected for the 10% probability level, ranging from 159.9 mm (20.7%, Medium) to 185.0 mm (23.9%, High) for the 2050s and from 183.9 mm (23.8%, Low) to 230.4 mm (29.8%, High) for the 2080s.

Figure 3 shows marked seasonal variations in projected changes in precipitation that vary between scenarios. For the 2050s, the two most extreme probability scenarios project year-round declines (10% probability) and increases (90% probability) in precipitation. This is nearly repeated for the 2080s apart from small (≤3%) increases in February precipitation (for 2080M$_{10}$ and 2080H$_{10}$) and even smaller (0.2%) declines in August (2080M$_{90}$). Progressively more months are projected to experience gains in precipitation with increasing probability level. For example, between 3 and 4 (5 for the

2080s) months, centred on January/February, experience higher precipitation for the 30% probability level. This increases to 5–7 (2050s) and 6–7 (2080s) for the 50% probability level. For the 70% probability level scenarios, projected declines in monthly mean precipitation are largely restricted to the summer months of July–September. As with annual precipitation, the magnitude of changes in monthly precipitation generally, although not exclusively, increase from Low, through Medium to High emission scenarios, with changes in the 2080s generally exceeding those for the 2050s. For example, precipitation in November, which under baseline conditions is the wettest month (84.9 mm) is, for the central (50%) probability level in the 2050s, projected to increase by 4.4, 9.6 and 11% for the Low, Medium and High emission scenarios, respectively. Extreme (Low and High) changes for this probability level in the 2080s are associated with increases of 13.2 and 15.2%, respectively. The same trend is evident in the summer declines in precipitation that are projected for most scenarios. The largest absolute and percentage declines occur in August. For the 50% probability level these vary between 19.8% (Low) and 30.4% (Medium) for the 2050s and from 23.9% (Low) and 40.2% (High) for the 2080s.

The uncertainty in the direction of change that is evident for precipitation is largely absent for PET. Table 1 shows that whilst the 10% probability level produces declines in annual PET for all three emission scenarios in both time slices, these changes are very small (no more than 9.4 mm or 1.8% of the 509.0 mm baseline). Beyond this probability level, annual PET increases for all scenarios. The magnitude of these changes progressively increases with higher probability level, emission scenario and future time slice. For the central (50%) probability level annual PET increases by between 55.4 mm (10.9%, Low) and 64.2 mm (12.6%, High) in the 2050s. The corresponding range for the 2080s is 63.7–92.3 mm (12.5–18.1%). Changes very unlikely to be exceeded (90% probability level) range over 128.9–147.9 mm (25.3–29.1%) for the 2050s and 147.6–210.1 mm (29.0–41.3%) for the 2080s. Beyond the 10% probability level, which tends to produce small declines in summer months and even smaller increases when baseline PET is low, mean monthly PET increases through most of the year (Fig. 3). The exceptions to this are PET declines projected for December and/or January for many scenarios, although, given the very low PET at this time, these changes are extremely small in real terms. Some of the largest absolute and percentage increases in PET are projected for the summer months of June–August, which under baseline conditions experience the largest monthly PET totals. For example, increases in August (baseline PET: 70.9mm) for the 50% probability level
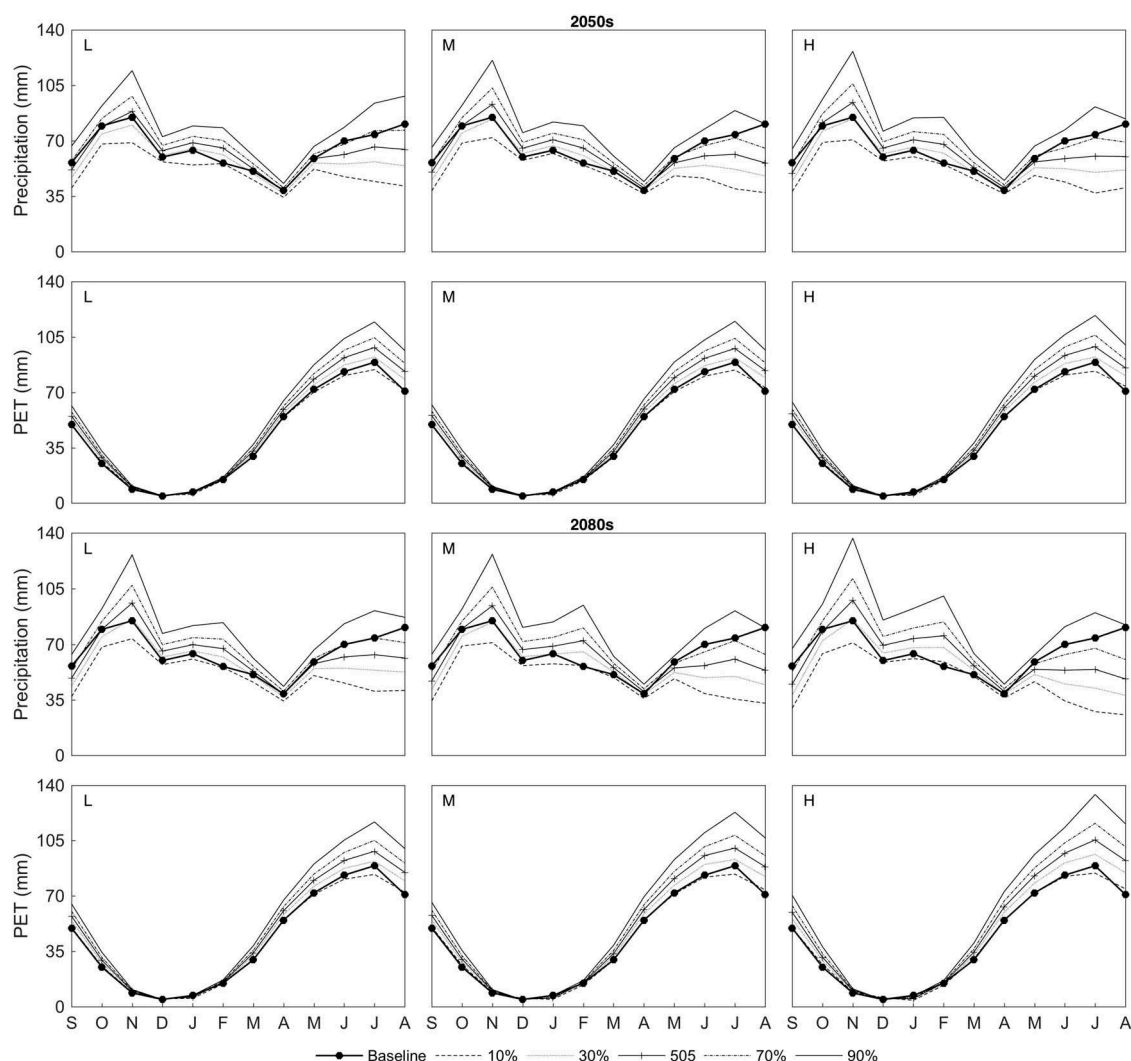
Figure 3. Mean monthly precipitation and potential evapotranspiration for the baseline and each UKCP09 scenario for the 2050s and 2080s.

range over 12.4–14.6 mm (17.5–20.7%) for the 2050s and 14.1–21.5 mm (19.8–24.8%) for the 2080s.

An initial indication of the likely hydrological impacts of the changes in precipitation and PET discussed above is provided in the bottom half of Table 1. Mean annual net precipitation (precipitation – PET) for the baseline and each scenario are shown. The number of months (and percentage of the 120 months for which data are available) when net precipitation is positive is also provided for the baseline and scenarios. Annual net precipitation does suggest a dominant drying trend for the climate change scenarios. With the exception of changes that are very unlikely to be exceeded (i.e. the 90% probability level), annual net precipitation declines from the baseline of 264.2 mm for all scenarios (Table 1). For a given time slice and emission scenario, the magnitude of these reductions declines with higher probability level, whilst in most

cases there is a consistent increase in the size of the reductions (i.e. lower net precipitation) from Low, through Medium to High emission scenario. The 2080s are associated with larger reductions in net precipitation than the 2050s. At the extreme low probability (10%) level, the magnitudes of the reductions range between 154.7 mm (58.6%) and 165.0 mm (62.5%) for the 2050s and 156.6 mm (59.3%) and 208.4 mm (78.9%) for the 2080s. The smaller reductions for the 50% probability level range between 69.3 mm (26.2%) and 78.8 mm (29.8%) for the 2050s. The corresponding figures for the 2080s are 73.6 mm (27.9%) and 119.4 mm (45.2%). These reductions are larger than the increases projected for the 90% probability level: 2050s: 27.3 mm (M) to 41.6 mm (L) (10.3–15.7%); 2080s: 18.5 mm (M) to 36.3 mm (L) (7.0–13.7%).

Despite the increases in mean annual net precipitation for the 90% probability level scenarios, the

incidence of positive monthly net precipitation throughout the simulation period declines for all 30 of the climate change scenarios. At the 90% probability level, these reductions are relatively small; 1 month for the Low emission scenario in both the 2050s and 2080s increasing to 2 (2050s) and 6 (2080s) months for the High emission scenario. At the other extreme (10% probability), the incidence of positive net precipitation declines by between 10 (Low) and 13 (Medium) months for the 2050s and between 11 (Low) and 14 (Medium and High) months in the 2080s. The central (50%) probability level is associated with reductions in the number of months with positive net precipitation of between 5 and 8 (Low and High, respectively) for the 2050s and 7 and 13 (again for the Low and High emission scenarios) for the 2080s.

Scenario River Glaven discharge

Observed and MIKE NAM simulated discharges of the River Glaven at Hunworth for the period 2001–2010 are shown at both daily and monthly resolutions in Figure 4. Seasonality in baseflow and timing of flood events is clearly reproduced at the daily resolution (Fig. 4 – top), although the magnitude of individual floods does tend to vary between observed and simulated discharges. An approximately equal number of events are overestimated and underestimated. This may result from temporal variations in runoff characteristics that cannot be represented within the model and result from the inherent patchiness of the largely

agricultural landscape and its impacts on hydrological behaviour (see for example Fiener et al. 2011). As a result, whilst the value of bias (Dv: 0.19%) is classified as "excellent" according to the model performance classification scheme of Henriksen et al. (2008), NSE (0.57) is classed as "fair". The value of the Pearson correlation coefficient (r), which is not included in the performance classification scheme, is 0.76. The impact of differential representation of peak events is largely removed when observed and simulated discharges are compared at a monthly time step (Fig. 4 – bottom). Values of DV, NSE and r are 0.20% ("excellent"), 0.768 ("very good") and 0.881, respectively. Since the discharge delta factors approach is based on differences between baseline and scenario mean monthly discharges simulated by NAM, model performance is considered sufficient to enable its use in deriving perturbed River Glaven discharge for the climate change scenario using the approach described above.

The impact of the UKCP09 climate change scenarios upon the discharge of the River Glaven at Hunworth is summarized in Table 2. This shows the mean, Q5 and Q95 (exceeded 5 and 95% of the time, respectively) discharges for the baseline and each scenario for the period 2001–2010. The dominant trend of declining discharge is clearly evident, especially for the high (Q5) and low (Q95) discharges that decline for all the scenarios except those of the 90% probability level. Whilst mean discharge increases for three 70% probability level scenarios, the magnitudes of these
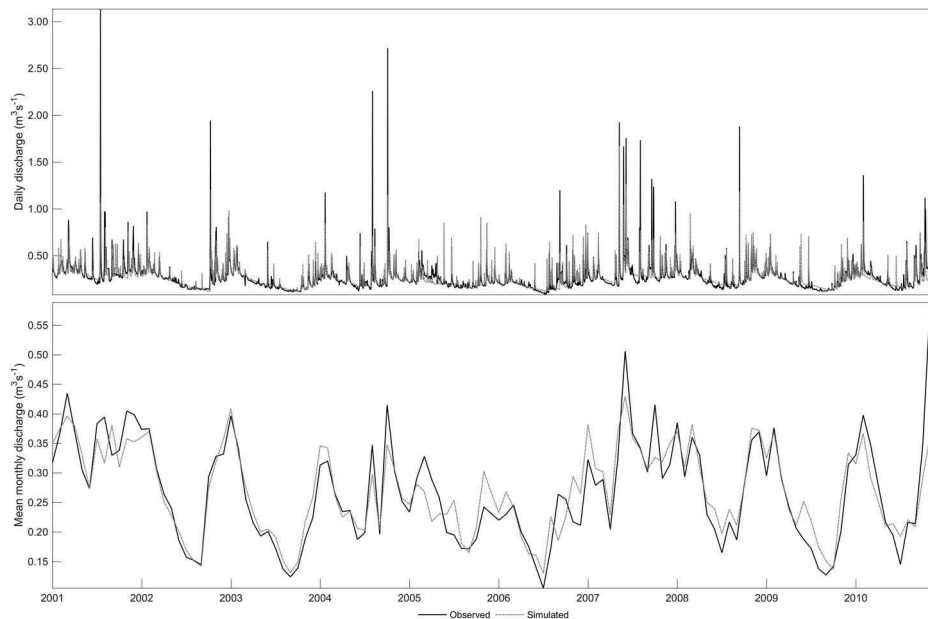

Figure 4. Observed and MIKE NAM simulated mean daily and mean monthly discharge at the Hunworth gauging station for the period 2001–2010.

Table 2. Baseline and UKCP09 scenario mean, Q5 and Q95 discharges ($m^3 s^{-1}$) and frequency of discharge exceeding post-restoration discharge thresholds associated with widespread (1.67 $m^3 s^{-1}$) and localized (0.60 $m^3 s^{-1}$) inundation. Frequency is specified as days for both thresholds (and number of discrete events for localized inundation). Shaded cells indicate reductions compared to the baseline. Data are based on the period 2001–2010.

		10%	30%	50%	70%	90%
Q5 discharge: Baseline 0.499						
2050s	L	0.330	0.390	0.437	0.494	0.600
	M	0.331	0.388	0.434	0.487	0.582
	H	0.322	0.387	0.439	0.499	0.603
2080s	L	0.329	0.391	0.440	0.498	0.600
	M	0.312	0.374	0.425	0.486	0.596
	H	0.300	0.396	0.420	0.488	0.621
Mean discharge: Baseline 0.278						
2050s	L	0.184	0.219	0.247	0.280	0.337
	M	0.183	0.217	0.244	0.275	0.330
	H	0.178	0.216	0.246	0.280	0.341
2080s	L	0.182	0.219	0.248	0.281	0.339
	M	0.171	0.208	0.238	0.273	0.335
	H	0.163	0.219	0.232	0.272	0.348
Q95 discharge: Baseline 0.137						
2050s	L	0.078	0.097	0.112	0.131	0.163
	M	0.075	0.093	0.107	0.124	0.154
	H	0.073	0.092	0.108	0.126	0.158
2080s	L	0.075	0.094	0.110	0.128	0.159
	M	0.068	0.086	0.102	0.120	0.153
	H	0.064	0.088	0.096	0.117	0.157
Widespread inundation threshold exceedence: Baseline 8						
2050s	L	1	2	4	7	10
	M	1	2	4	7	10
	H	1	2	4	7	10
2080s	L	1	2	4	8	10
	M	1	2	3	5	10
	H	1	3	3	5	10
Localised inundation threshold exceedence: Baseline 97 (57)						
2050s	L	29 (20)	42 (28)	65 (40)	97 (55)	173 (85)
	M	28 (19)	41 (28)	61 (37)	94 (54)	160 (82)
	H	25 (19)	41 (28)	63 (38)	101 (56*)	175 (87)
2080s	L	29 (20)	42 (29)	67 (40)	103 (57)	174 (87)
	M	21 (18)	34 (23)	54 (34)	89 (51)	170 (86)
	H	16 (15)	44 (29)	51 (33)	89 (51)	197 (94)

* Whilst the number of days when the localized inundation discharge threshold is exceeded increases compared to the baseline, the number of discrete events associated with discharges above this threshold declines.

increases are very small and of a similar size as declines projected by the other three scenarios of this probability level (total range: −2.2 to 1.0%). For the central probability level (50%) declines in mean discharge vary between 11.2% (Low) and 12.2% (Medium) for the 2050s and between 10.8% (Low) and 16.5% (High) for the 2080s. Much larger declines are projected for the lowest probability (10%) level: 33.8–36.0% and 34.5–41.4% for the Low and High emission scenarios in the 2050s and 2080s, respectively. At the other extreme, the increases in mean discharges that are very unlikely to be exceeded (90% probability level) range over 18.7–22.7% and 20.5–25.2% (Medium and High for the 2050s and 2080s, respectively). The magnitudes of the changes in peak (Q5) discharges are, in percentage terms, very similar to those for the mean. The largest percentage difference between change in Q5 and mean discharge for a given scenario is less than 2.0%. The central probability scenarios project declines in Q5 of between 12.0% (High) and 13.0%

(Medium) for the 2050s and between 11.8% (Low) and 15.8% (High) for the 2080s. In percentage terms, changes in Q95 discharge are larger (by on average 9.4%) than those for mean discharge although absolute changes are relatively small. Q95 discharges for the central (50%) probability level decline by between 18.2% (Low) and 21.9% (Medium) for the 2050s whilst for the later time slice larger declines of between 19.7% (Low) and 29.9% (High) are projected. The largest declines are projected for the 10% probability level (43.1–46.7% and 45.3–53.3% for the Low and High emission scenarios in the 2050s and 2080s, respectively). In contrast, the increases in low flows projected by the 90% probability level are smaller (total range 11.7–19.0% for the 2080M_{90} and 2050L_{90} scenarios, respectively).

Baseline and scenario mean monthly discharges further illustrate the impacts of the UKCP09 projections (Fig. 5). Year-round reductions in monthly mean discharges are projected for all probability levels
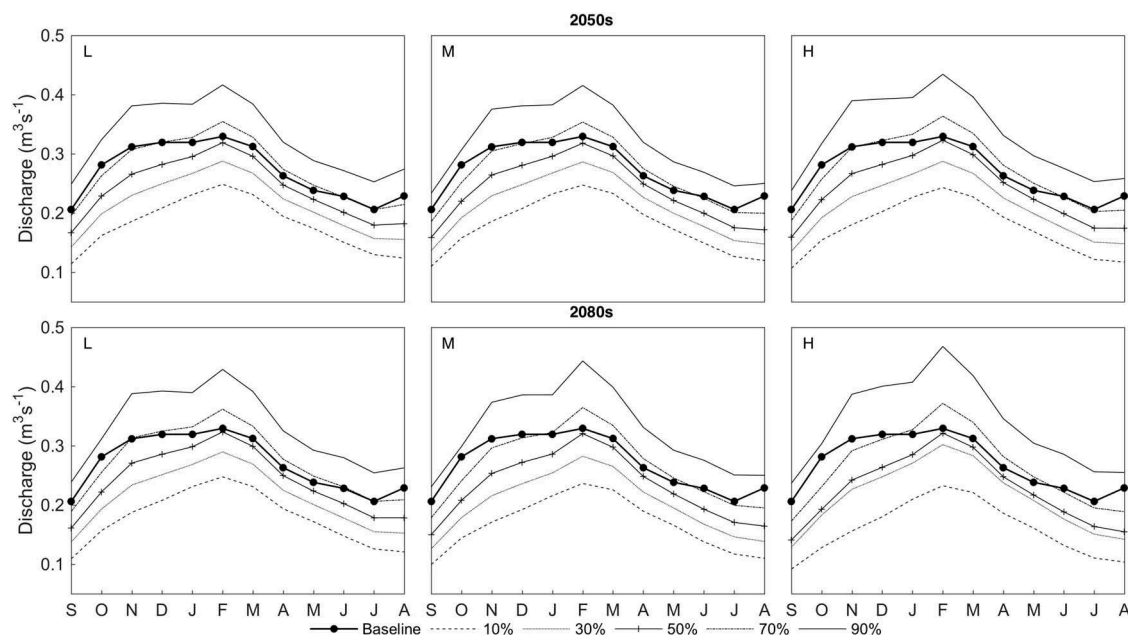
Figure 5. Mean monthly discharge at Hunworth simulated by the NAM model for the baseline and each UCKIP09 scenario for the 2050s and 2080s.

below and including 50% for all emission scenarios and both time slices. The magnitudes of these reductions tend to increase with emission scenario (from Low, through Medium to High) and are, in general, larger in the 2080s compared to the 2050s. For these scenarios, the relatively high discharges in mid-winter (November–January) are reduced more than those of the seasonal peak (0.329 m³ s⁻¹) in February. For example, the mean discharge in February declines by only 3.5% for 2050M$_{50}$, whilst discharges in the three previous months are reduced by between 7.4 and 15.3%. The corresponding reductions for 2080M$_{50}$ are 2.7% (February) and 10.4–18.8% (November–January). Summer discharges are, in percentage terms, reduced even more, reflecting the larger reductions in Q95 discussed above. For example, on average the discharges in August and September decline by 24.0 and 27.7% for 2050M$_{50}$ and 2080M$_{50}$, respectively. For the 10% probability level these declines are as large as 48.5% (compared to 26.2% for the seasonal peak) for 2050H$_{10}$ and 55.1% (compared to 29.4%) for 2080H$_{10}$. For the 70% probability level, winter discharges increase whilst summer low flows decline. The number of months experiencing higher discharges does vary between scenarios, with the increase in the February peak ranging between 7.4% (2050M$_{70}$) and 12.1% (2080H$_{70}$). All 90% probability scenarios project year-round increases in monthly mean discharges, with the largest absolute and percentage increases projected for February. For the

2050s these range between 26.2 and 26.4% (Medium and Low, respectively) to 31.9% (High). Increases are larger for the 2080s, ranging between 30.3% (Low) and 42.1% (High).

A preliminary assessment of the impacts of changes in river discharge upon flooding of Hunworth Meadow is possible by comparing baseline and scenario discharge time series with estimates of channel capacity identified by Clilverd et al. (2016). During the period 2001–2010, the observed baseline daily discharge at Hunworth never exceeded the estimated pre-restoration channel capacity of 5.1 m³ s⁻¹. This is repeated for all scenario discharge time series, suggesting that, in the absence of embankment removal, overbank inundation would be little impacted by climate change. However, changes from the baseline are evident in the frequency at which lower post-restoration threshold discharges are exceeded. The first of these thresholds (1.67 m³ s⁻¹) corresponds to the bankfull channel capacity that, once exceeded, leads to potentially widespread inundation whilst the second smaller threshold (0.6 m³ s⁻¹) is associated with localized inundation along the river margin. Table 2 summarizes the frequency of these thresholds being exceeded for the baseline and each climate change scenario during the 2001–2010 simulation period. In the case of the higher bankfull threshold, periods of exceedence are limited to a single day. However, the lower threshold is in some cases exceeded for a number of days during any one event. Table 2 therefore shows the total number of days

as well the number of discrete events when this threshold is exceeded. The latter is defined as a period when discharge is consistently above 0.6 m^3 s^{-1}.

The pattern of change in the frequency of post-restoration bankfull discharge exceedence under the different climate change scenarios follows that of the Q5 discharge, with the 10–70% probability level scenarios experiencing potential declines in widespread inundation (the exception being 2080L$_{70}$ with no change). The number of events that exceed this threshold discharge declines with a reduction in probability level and for a given level is relatively consistent. The 50% probability level is associated with around a halving of events likely to lead to overbank inundation, whilst all of the 10% probability level scenarios led to only one such event compared to eight for the baseline. At the other extreme, a further two events exceed bankfull channel capacity for all the 90% probability level scenarios. A similar pattern is evident for the 0.6 m^3 s^{-1} threshold discharge, although there is a little more uncertainty in the direction of change for the 70% probability level. The number of days (events) when this threshold is exceeded declines by between 30.9 and 47.4% (29.8–42.1%) for the central 50% probability level, and by 70.1 and 83.5% (64.9–73.7%) for the 10% probability level. The largest declines are predominantly associated with the higher emission scenarios and later time slice. As with the bankfull threshold, the 90% probability level scenarios produce potential increases in the frequency of localized flooding. The number of days (events) when this threshold discharge is exceeded increases by between 64.9 and 103.1% (43.9–64.9%). The notably largest increases are associated with the 2080H$_{90}$ scenario.

Floodplain groundwater levels

Figures 6 and 7 show MIKE SHE simulated daily water table elevations at the location of two of the shallow wells installed within Hunworth Meadow (see Fig. 1 for locations). For clarity, results are shown for the baseline and the 10, 50 and 90% probability levels for each UKCP09 scenario and the two time slices. Simulated water table elevations for intervening probabilities (i.e. 30 and 70%; not shown) lie approximately mid-way between those of adjacent probabilities (see also Thompson 2012). The selected wells are representative of climate scenario-driven changes in groundwater elevation across the majority of the floodplain (Well 1.4) as well as close to the River Glaven (Well 1.1), although absolute elevations vary following the shallow downstream topographic gradient of the ground surface (Clilverd et al. 2016). This is evident in Figure 8,

which shows mean monthly water table elevations derived from the complete simulation period for the same two wells and two additional wells located at approximately the same position across the floodplain (Well 3.1 close to the river, Well 3.2 on the floodplain) but towards the upstream end of Hunworth Meadow (see Fig. 1).

As discussed by Clilverd et al. (2016), whilst strong seasonality in simulated groundwater elevation is evident throughout Hunworth Meadow under baseline conditions, the water table is considerably more variable over short timescales close to the river (Fig. 6) compared to the majority of the floodplain (Fig. 7). As shown in Figure 8, baseline mean monthly water table elevation at Well 3.1, installed at the location of the former embankment where the ground surface was lowered following restoration, is above the ground surface between November and February. Although Well 1.1 is also close to the river, it was not subject to ground surface level changes following embankment removal. While baseline water table elevation is high during these 4 months, it is on average 0.10 m below the ground surface (Fig. 8). Groundwater does, however, regularly reach the surface in response to individual rain/river flow events (Fig. 6). Further away from the river, the influence of individual events tends to diminish and short-term variations in water table elevation are much smaller. This is clearly shown at Well 1.4 located towards the lowest part of the floodplain, where on average under baseline conditions the water table is at the ground surface between December and February (Fig. 8) and in some years for extended periods (Fig. 7). Short-lived peaks when the baseline water table elevation is above the ground surface coincide with the flood events that exceed the post-restoration bankfull channel capacity (Table 2). These events also impact groundwater levels further upstream on the floodplain (e.g. Well 3.2), although the higher ground surface elevation results in the water table elevation oscillating between being at and below the surface during the winter months, with the result that on average it is just over 0.09 m below the ground surface between December and February (Fig. 8).

The distinctions between water table elevation close to the river and beneath the wider floodplain are retained in the results for the UKCP09 scenarios (Figs 6 and 7). Echoing the scenario changes in precipitation and PET and, in turn, river discharge, a dominant trend towards lower groundwater level is apparent at both sets of locations. Differences between baseline and scenario groundwater levels are generally larger beyond the immediate influence of the river (e.g. Well 1.4; Fig. 7), with the largest changes projected
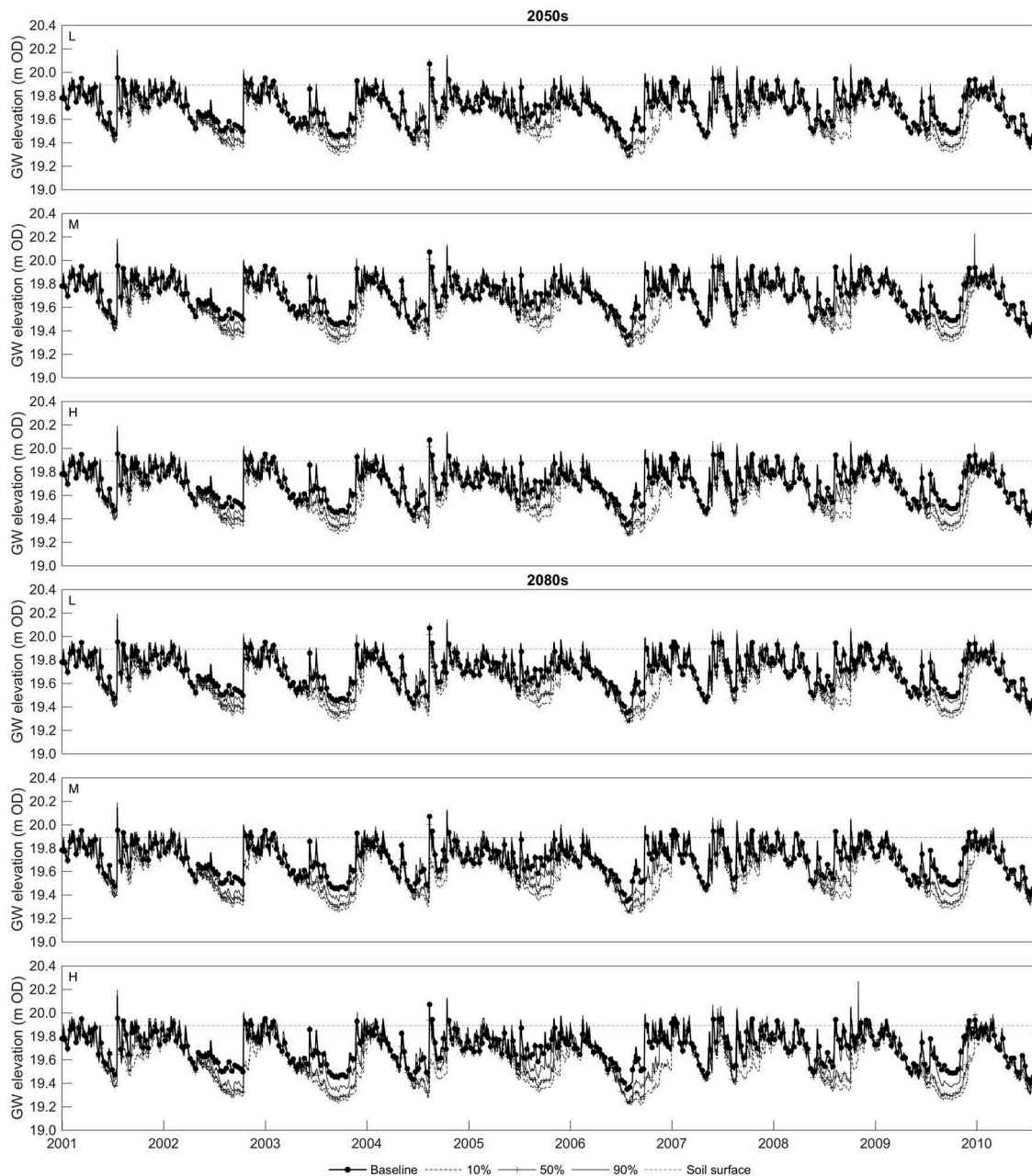
Figure 6. Simulated daily water table elevation at Well 1.1 for the baseline and selected UKCP09 scenarios for the 2050s and 2080s.

during the summer drawdowns. The magnitude of these summer declines in water table elevation does vary markedly from year to year. Using Well 1.4 as an example of changes across the floodplain beyond the riparian area, the largest individual declines in daily water table elevation occur in late September 2006. For the 2050s, the largest declines at this time for the 10% probability level range between 0.89 m (L_{10}) and 0.93 (H_{10}), whilst the corresponding range for the 2080s is 0.92–1.04 m. This probability level is particularly notable in delaying the autumn rise in water table in this year, a feature that is repeated in a number of other years (e.g. 2003, 2009). Reductions for the 50%

probability level are still relatively large (2050s: 0.75–0.85 m; 2080s: 0.88–1.01 m) and only the 90% probability level (70% also for 2050L) projects increases at this time although these are very small (all < 0.05 m). In contrast, in some years (e.g. 2001 and 2007) that, under baseline conditions, experience relatively wet summers, declines in water table elevation are considerably smaller. For example, in 2001 the largest declines in summer water table elevation at Well 1.4 for a specific scenario are less than a quarter the magnitude of those experienced in 2006. Inter-scenario differences in the highest groundwater elevations are much less evident than those for the lowest elevations
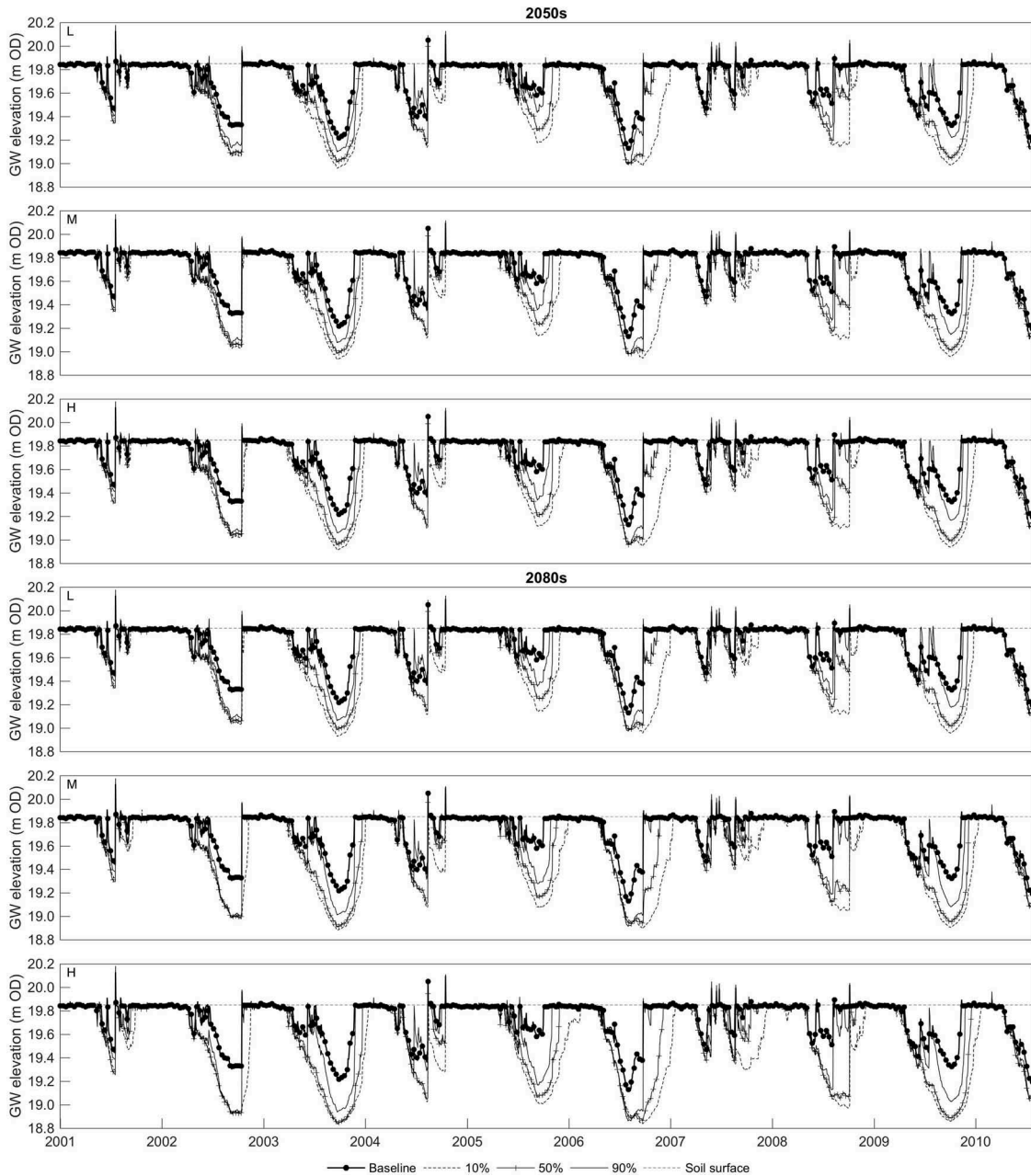
Figure 7. Simulated daily water table elevation at Well 1.4 for the baseline and selected UKCP09 scenarios for the 2050s and 2080s. Note that whilst the absolute *y*-axis ranges differ from the corresponding figure for Well 1.1 shown in Fig. 6 they covers the same range.

(Fig. 7). At Well 1.4 the water table still reaches the ground surface in all years in each scenario although, as noted previously, it does so progressively later for the lower probability levels.

The mean monthly water table elevations for Well 1.4 (Fig. 8) summarize these impacts. Declining groundwater levels are projected between at least April and November for all scenarios in both time slices. The period of declining water table elevations expands as probability level declines, with all 10% probability level scenarios projecting declines in

every month, although declines in the middle of winter are very small. For a given emission scenario and time slice the magnitude of the reduction in water table level clearly increases as probability level declines. Similarly, larger reductions tend to be associated with the higher emission scenario and more distant time slice. For example, the largest reductions consistently occur in September, and for 2050M these vary between 0.13 m (90% probability) and 0.36 m (10% probability). For the 50% probability level and this time slice, reductions increase from 0.20 m
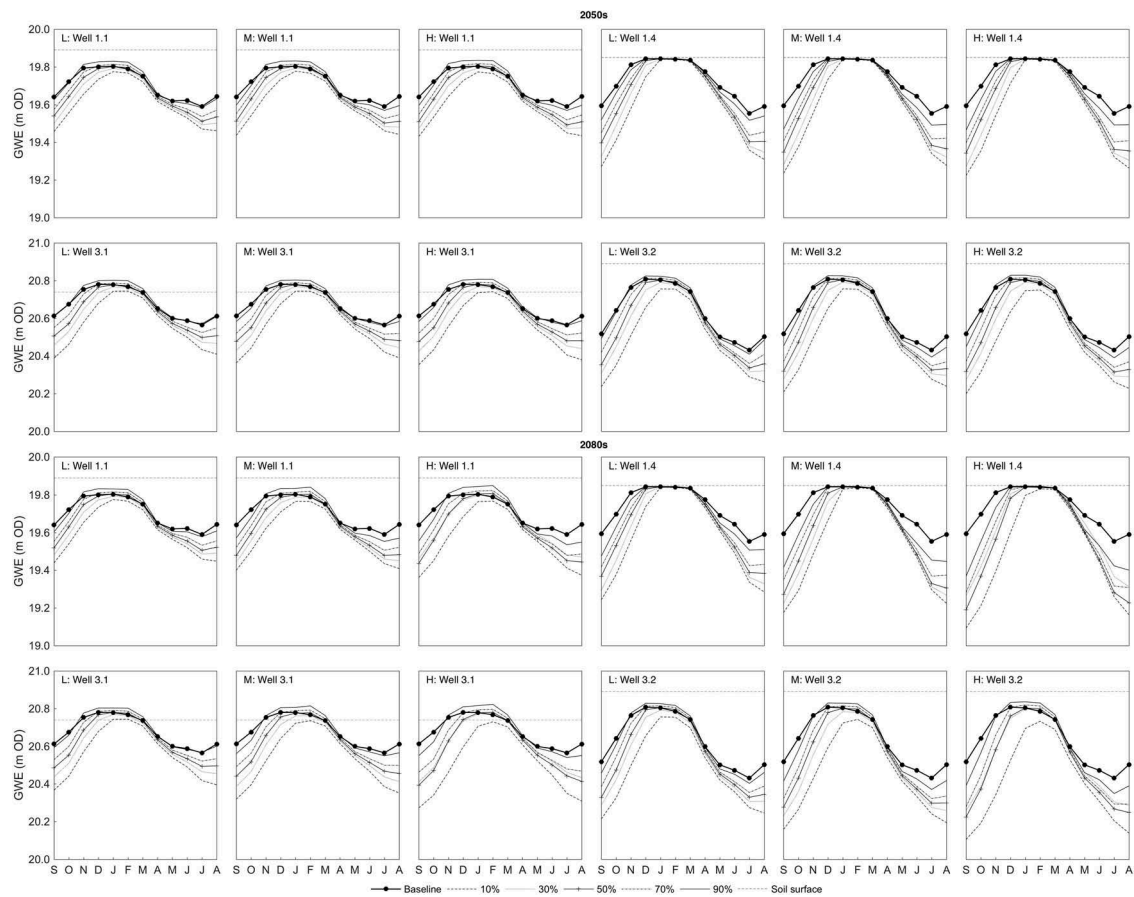
Figure 8. Simulated mean monthly water table elevation at four shallow wells within Hunworth Meadow for the baseline and each UKCP09 scenario for the 2050s and 2080s. Note that whilst the absolute y-axis ranges vary between wells at the downstream (Wells 1.1 and 1.4) and upstream (Wells 3.1 and 3.2) ends of the floodplain, they cover the same range.

(Low), through 0.24 m (Medium) to 0.25 m (High), with the corresponding range for the 2080s being 0.23–0.40 m. These trends are replicated in the figures for WTE-95 (the water table elevation exceeded for 95% of the complete simulation period) for Well 1.4 (Table 3). The dominant drying trend is further emphasized by the consistent reduction in mean water table elevation (Mean WTE) for all scenarios and by the fact that in the vast majority of scenarios (the exception being 2050L$_{90}$), over 50% of the simulated daily water table elevations decline from the baseline. Reductions from the baseline mean of 19.73 m OD range between 0.03 m (L90) and 0.16 m (H10) for the 2050s, with the corresponding range being 0.04 and 0.23 m for the 2080s. The very limited changes in the high water table elevations are demonstrated by the near consistent WTE-5 (the water table elevation exceeded for 5% of the time; Table 3) across the scenarios. Projected reductions (10–50% probability levels) and increases (70% and 90% probability levels) remain below a centimetre in magnitude, so

that mean peak water table elevations in January–March are barely impacted (Fig. 8).

The same general patterns are evident in the mean monthly water table elevations at Well 3.2, the other well located on the floodplain at a distance from the river (Fig. 8), although there are some minor differences in the changes in winter peaks. Since, as outlined above, baseline water table elevations at this time of year vary between being at and just below the ground surface, the wetter winters projected by higher probability level scenarios do result in a slight increase in mean monthly water table elevations in a number of winter months (up to six, November–March for the 90% probability level scenarios). This is linked to an increase in the level to which the water table periodically falls after periods when it reaches the surface, rather than to substantial increases in the latter peaks. These changes are, however, much smaller (largest: 0.03 m for 2080H$_{90}$) than the declines in summer. Unlike the results for Well 1.4, the delayed rise in autumn groundwater levels for

Table 3. Simulated baseline and UKCP09 scenario 5-percentile (WTE-5), mean and 95-percentile (WTE-95) water table elevations (WTE; m above OD) and number of days (%, to the nearest integer of the total 3493 days) when scenario water table elevation is below baseline water table elevation at the location of two representative shallow wells within Hunworth Meadow. Shaded cells indicate reductions in water table elevation compared to the baseline and scenarios when over 50% of days experience lower water table elevations than the baseline.

		2050s					2080s				
		10%	30%	50%	70%	90%	10%	30%	50%	70%	90%
Well 1.1											
WTE-5: Baseline 19.91											
	L	19.86	19.89	19.90	19.92	19.94	19.86	19.89	19.91	19.92	19.94
	M	19.86	19.89	19.90	19.92	19.94	19.85	19.89	19.90	19.92	19.94
	H	19.86	19.89	19.90	19.92	19.94	19.85	19.90	19.90	19.92	19.94
Mean WTE: Baseline 19.70											
	L	19.61	19.64	19.66	19.68	19.71	19.60	19.63	19.65	19.67	19.70
	M	19.61	19.63	19.65	19.67	19.70	19.59	19.62	19.64	19.66	19.69
	H	19.60	19.63	19.65	19.67	19.70	19.57	19.63	19.62	19.65	19.69
WTE-95: Baseline 19.48											
	L	19.34	19.36	19.38	19.41	19.45	19.33	19.35	19.37	19.39	19.44
	M	19.32	19.35	19.37	19.39	19.43	19.30	19.32	19.34	19.36	19.40
	H	19.32	19.34	19.36	19.38	19.43	19.27	19.35	19.31	19.33	19.38
Days (% of 3493 total) when scenario WTE < baseline WTE											
	L	3467 (99)	3301 (95)	2870 (82)	2177 (62)	1340 (38)	3472 (99)	3275 (94)	2725 (78)	2184 (63)	1545 (44)
	M	3464 (99)	3296 (94)	2787 (80)	2181 (62)	1537 (44)	3478 (100)	3252 (93)	2833 (81)	2197 (63)	1737 (50)
	H	3476 (100)	3270 (94)	2723 (78)	2134 (61)	1504 (43)	3467 (99)	2935 (84)	2761 (79)	2218 (63)	1769 (51)
Well 1.4											
WTE-5: Baseline 19.85											
	L	19.85	19.85	19.85	19.85	19.86	19.85	19.85	19.85	19.85	19.86
	M	19.85	19.85	19.85	19.85	19.86	19.85	19.85	19.85	19.85	19.86
	H	19.85	19.85	19.85	19.85	19.86	19.85	19.85	19.85	19.85	19.86
Mean WTE: Baseline 19.73											
	L	19.59	19.62	19.65	19.67	19.70	19.58	19.61	19.64	19.66	19.69
	M	19.58	19.61	19.63	19.66	19.69	19.54	19.58	19.60	19.63	19.67
	H	19.57	19.60	19.63	19.65	19.69	19.50	19.61	19.57	19.61	19.65
WTE-95: Baseline 19.33											
	L	19.03	19.07	19.09	19.12	19.22	19.01	19.04	19.06	19.08	19.15
	M	19.00	19.04	19.06	19.08	19.14	18.96	18.98	19.00	19.02	19.08
	H	18.99	19.02	19.04	19.07	19.13	18.90	19.03	18.93	18.94	19.02
Days (% of 3493 total) when scenario WTE < baseline WTE											
	L	3253 (93)	3017 (86)	2739 (78)	2326 (67)	1707 (49)	3244 (93)	2977 (85)	2690 (77)	2337 (67)	1830 (52)
	M	3239 (93)	2996 (86)	2683 (77)	2343 (67)	1906 (55)	3275 (94)	2997 (86)	2720 (78)	2400 (69)	2036 (58)
	H	3273 (94)	2983 (85)	2657 (76)	2300 (66)	1841 (53)	3228 (92)	2742 (78)	2727 (78)	2449 (70)	2026 (58)

the lowest probability level (10%) scenarios means that winter peak levels are more obviously lower than under baseline conditions.

Whilst very similar overall patterns of change in scenario water table elevation are simulated for riparian wells as those on the floodplain, the proximity of the river does reduce the magnitude of declines in summer groundwater elevations (contrast Well 1.1 [Well 3.1] with Well 1.4 [Well 3.2] in Figs 6–8). For example, the September declines in mean water table elevation at Well 1.1 for the 2050s Medium emission scenario vary between 0.04 m (90% probability) and 0.20 m (10% probability), considerably smaller than those previously reported for Well 1.4 (0.13 m and 0.36 m, respectively). Similarly, the Low, Medium and High emission scenarios for this time slice and the 50% probability level induce mean declines in September of 0.10, 0.11 and 0.12 m, respectively (0.20, 0.24 and 0.25 m for Well 1.4). The same range for the 2080s is similarly reduced to 0.12–0.20 m (from 0.23–0.40 m). WTE-95 declines for all scenarios (Table 3). Proximity to the river also leads to more obvious increases in mean monthly water tables in winter at Wells 1.1 and 3.1 compared to those further from the river (Fig. 8). These increases are, however, still small in comparison to the declines in summer, the largest for Well 1.1 being 0.06 m in February for $2080H_{90}$, and are restricted to probability levels of at least 50% (30% in the case of 2080H). WTE-5 at Well 1.1 increases for the same scenarios as at Well 1.4, although again, changes are very small as are the declines for the other scenarios (Table 3). Mean WTE at Well 1.1 increases for only one of the highest probability level scenarios ($2050L_{90}$), albeit by less than a centimetre. It is unchanged for three and declines (by less than a centimetre) for the other two high probability (90%) scenarios. With the exception of $2080M_{90}$ and $2080H_{90}$, the 90% probability scenarios project higher daily water table elevations compared to baseline for over 50% of the simulation period. All of the other scenarios project declines in daily water table elevation for the majority of this period.

Floodplain inundation

Given the reported dominance of declines in peak river flows, and in turn the reduction in the frequency at which discharges exceed channel capacities associated with flooding (Table 2), the majority of UKCP09 scenarios project declines in flood extent within the restored floodplain of Hunworth Meadow. The changing number of events when threshold channel capacities are exceeded for the different scenarios influences

direct comparisons, but an indication of the impacts can be established using the eight events when baseline river discharge exceeded the 1.67 m^3 s^{-1} threshold that is required for widespread inundation. For all three emission scenarios and both time slices, declines in total flood extent compared to the baseline are projected for the 10–70% probability levels. The magnitude of the declines generally increases with lower probability level, higher emission scenario and later time slice. In percentage terms, there is considerable variability in the magnitude of the declines in flood extent for the different events within an individual scenario. For example, the largest mean percentage decline in flood extent for the eight events (56.9%) is projected by $2080H_{10}$, although the decline for an individual event varies between 23.5 and 78.2%. $2050L_{70}$ projects the smallest mean decline (8.4%) with an inter-event range of 0.8–18.8%. For the 90% probability level scenarios, the direction of change in flood extent varies between events, with between one and five of the eight events increasing in flood extent for an individual scenario. The magnitude of the changes in either direction is relatively small, ranging between −7.2 and 5.4% across all 30 scenarios.

The impacts of the UKCP09 scenarios upon inundation within Hunworth Meadow can be illustrated in detail using the two flood events previously selected by Clilverd et al. (2016) to demonstrate the effects of embankment removal. The first event, which occurred on 18 July 2001, was the largest during the 10-year simulation period, with a baseline mean daily discharge of 3.1 m^3 s^{-1}. The second, smaller event (28 May 2007) was associated with a baseline mean daily discharge of 1.9 m^3 s^{-1}. For both events Figure 9 shows the simulated extent and depth of surface water under the baseline and the 10, 50 and 90% probability levels for the Medium emission scenario in the 2050s and 2080s. In common with the groundwater results, changes in inundation for the intervening probabilities (i.e. 30% and 70%) are approximately mid-way between the adjacent probabilities. This is demonstrated in Table 4, which provides the total flooded area for both events along with the extent of surface water with depths of <0.05 m, 0.05–0.4 m and >0.4 m for all scenarios and both time slices.

The total extent of inundation during the largest flood event of the simulation period for the 10 and 50% probability levels declines in both the 2050s and 2080s (Fig. 9). For the baseline, much of the Meadow is inundated, the exceptions being the isolated areas immediately adjacent to the river where embankments were not removed due to the presence of water vole burrows, and the far side of the floodplain where the
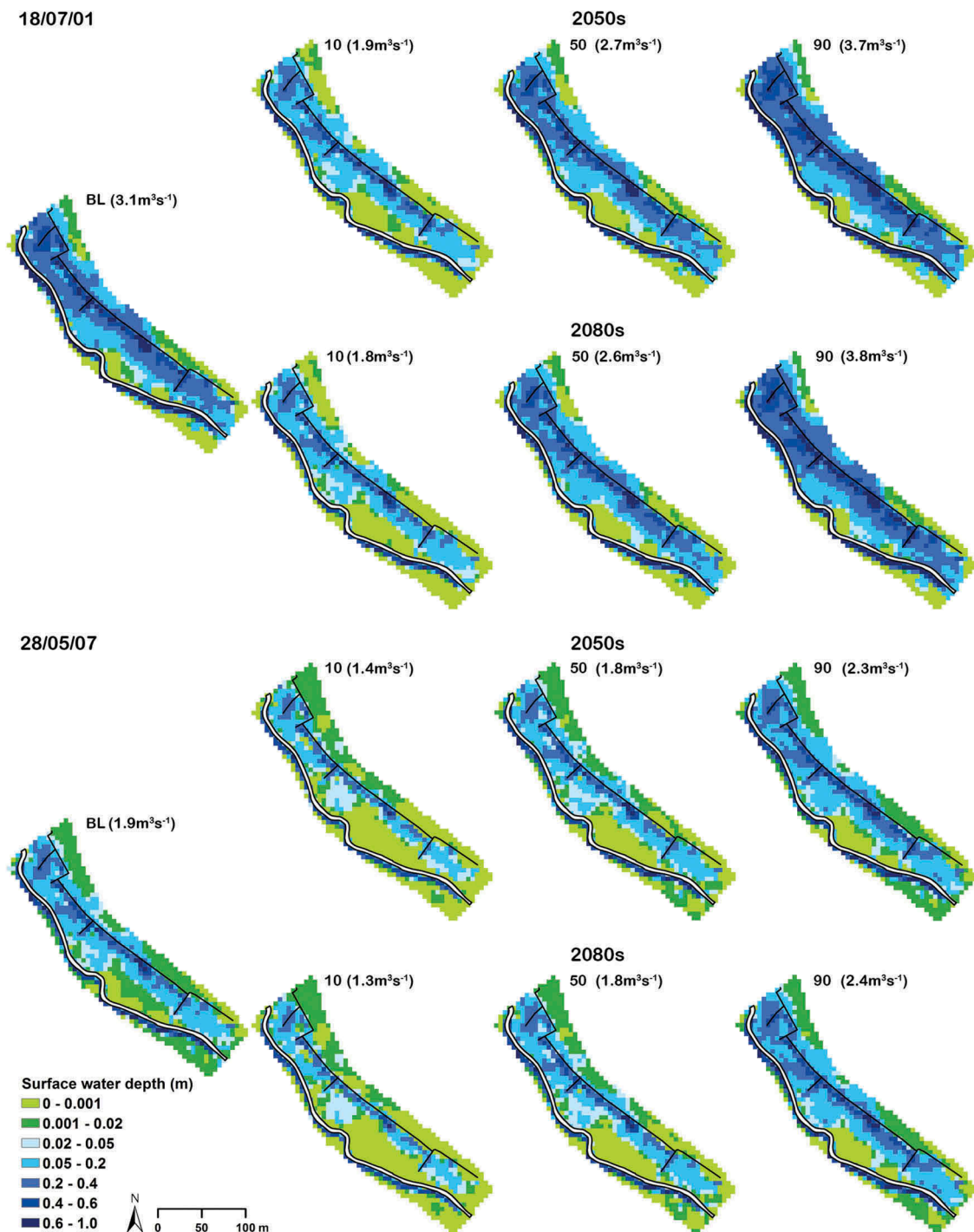
Figure 9. Simulated surface water extents and depths within Hunworth Meadow for the baseline and the Medium emission scenario and probability levels of 10, 50 and 90% for the 2050s and 2080s for two flood events. Discharge values refer to the baseline/scenario mean daily discharges on the date of the event.

surface elevation begins to increase towards the adjacent hillside. The extent of these areas expands with the lower probability levels, with the two dry riparian areas merging for the 10% probability scenarios in both time slices. The extent of the most deeply flooded areas constricts with a decline in probability level, and for 10% it is largely restricted to the MIKE SHE grid cells adjacent to the ditch that runs along the length of the floodplain. Conversely, at the highest (90%) probability level, the extent of this relatively deep water expands further away from the ditch compared to the baseline (Fig. 9). Total flood extent appears to increase marginally, with a few previously dry MIKE SHE grid cells now being inundated.

Table 4. Baseline and UKCP09 scenario total flooded area and extent of areas flooded to different depth range for two flood events (18 July 2001 and 28 May 2007). Discharge values refer to the baseline mean daily discharges on the date of the event.

			10%	20%	50%	70%	90%
18/07/2001 (3.1 m^3 s^{-1})	**Total flooded area: Baseline 21 300**						
	2050	L	18 225	19 275	20 150	21 125	21 950
		M	17 725	19 100	19 825	20 925	21 750
		H	17 225	18 925	19 750	20 925	21 850
	2080	L	17 675	19 175	20 025	21 050	21 875
		M	16 950	18 750	19 550	20 750	21 725
		H	16 300	19 025	19 025	20 350	21 700
	Flooded area < 0.05 m depth: Baseline 2675						
	2050	L	3500	2550	2425	2500	2175
		M	3350	2625	2300	2425	2050
		H	3150	2675	2225	2375	2050
	2080	L	3300	2575	2300	2425	2100
		M	3450	2725	2175	2250	1950
		H	3900	2775	2025	2100	1875
	Flooded area 0.05–0.4 m depth: Baseline 13 800						
	2050	L	11 675	13 100	13 500	13 800	13 450
		M	11 550	12 925	13 400	13 775	13 575
		H	11 300	12 725	13 400	13 800	13 450
	2080	L	11 550	13 025	13 525	13 800	13 450
		M	10 850	12 725	13 375	13 800	13 450
		H	9900	12 750	13 200	13 625	13 375
	Flooded area > 0.4 m depth (m^2): Baseline 4825						
	2050	L	3050	3625	4225	4825	6325
		M	2825	3550	4125	4725	6125
		H	2775	3525	4125	4750	6350
	2080	L	2825	3575	4200	4825	6325
		M	2650	3300	4000	4700	6325
		H	2500	3500	3800	4625	6450
28/05/2007 (1.9 m^3 s^{-1})	**Total flooded area: Baseline 24 375**						
	2050	L	16 600	19 250	20 925	22 350	23 600
		M	15 525	17 700	19 700	21 275	22 950
		H	15 100	17 625	19 625	21 475	22 925
	2080	L	15 850	18 325	19 925	21 625	22 875
		M	14 775	17 275	18 725	20 225	21 800
		H	13 425	18 375	18 050	19 500	21 625
	Flooded area < 0.05 m depth: Baseline 10 850						
	2050	L	7625	8450	8825	8400	7750
		M	6675	7075	7775	7400	7200
		H	6525	7050	7525	7300	7000
	2080	L	7050	7650	7800	7625	7025
		M	6400	6950	7000	6325	5925
		H	5700	7325	6500	5600	5425
	Flooded area 0.05–0.4 m depth: Baseline 10 850						
	2050	L	7200	8575	9650	11 200	12 625
		M	7075	8425	9475	11 150	12 550
		H	6825	8375	9650	11 400	12 625
	2080	L	7025	8475	9650	11 225	12 625
		M	6725	8225	9325	11 175	12 650
		H	6200	8775	9150	11 150	12 750
	Flooded area >0.4 m depth: Baseline 2675						
	2050	L	1775	2225	2450	2750	3225
		M	1775	2200	2450	2725	3200
		H	1750	2200	2450	2775	3300
	2080	L	1775	2200	2475	2775	3225
		M	1650	2100	2400	2725	3225
		H	1525	2275	2400	2750	3450

These changes are quantified in Table 4, which demonstrates that the total flooded area for the large event on 18 July 2001 declines from a baseline of 21 300 m^2 for all the scenarios except those with a 90% probability level. For a given emission scenario and time slice, declines in flooded area increase as probability level declines. Generally, although not exclusively, greater reductions in total flooded area are associated with higher emission scenarios and the later time slice. For example, the total area inundated for the central (50%) probability level in the 2050s is projected to decline by 1150, 1475 and 1550 m^2

(equivalent to 5.4, 6.9 and 7.3%) for the Low, Medium and High emission scenarios, respectively. These reductions increase in magnitude to 1275, 1750 and 2275 m^2 (6.0, 8.2 and 10.7%) for the 2080s. The 10% probability level scenarios induce declines in total inundation of between 3075 m^2 (14.4%, Low) and 4075 m^2 (19.3%, High) for the 2050s, with the corresponding range for the 2080s being 3625–5000 m^2 (17.0–23.5%). At the other extreme, the increases in total flood extent projected for the 90% probability level are relatively small, ranging between 450 m^2 (Medium) and 650 m^2 (Low) (2.1–3.1%) for the 2050s and from 400 m^2 (High) to 575 m^2 (Low) (1.9–2.7%) for the 2080s. At most, only an additional 26 MIKE SHE (5 m × 5 m) grid cells are inundated (for $2050L_{90}$) compared to the baseline.

The extent of very shallow (<0.05m) flooding during the large event is projected to decline for the vast majority of scenarios of 30% and above probability, exceptions being small reductions of 50 and 100 m^2 (or only two and four MIKE SHE grid squares) for $2080M_{30}$ and $2080H_{30}$, and no change for $2050H_{30}$ (Table 4). The largest reductions in total inundated area reported above for the 10% probability level scenarios are accompanied by increases in the extent of shallow flooding, which for the 2050s range between 475 m^2 (High) and 825 m^2 (Low) (17.8–30.8%) and for the 2080s between 625 m^2 (Low) and 1225 m^2 (High) (23.4–45.8%). In consequence, shallow flooding makes up a larger proportion of the total flooded area at low probability levels, whilst this proportion declines as probability level increases. For example, of the total area flooded for the $2050M_{10}$ scenario, 18.9% is less than 0.05 m deep compared to 12.6% for the baseline (Fig. 9). This declines to 11.6 and 9.4% for the $2050M_{50}$ and $2050M_{90}$, respectively. For the 2080s the corresponding figures are 20.4, 11.1 and 9.0%. The extent of inundation of between 0.05 and 0.4 m declines for all scenarios except four of the 70% probability level scenarios where it remains the same. The largest declines from the baseline are associated with the 10% probability level and range between 2125 and 2500 m^2 (15.4–18.1%) for the Low and High emission scenarios in the 2050s and between 2250 and 3900 m^2 (16.3–28.6%) for the same scenarios in the 2080s. The magnitude of the declines decreases towards the 70% probability level scenarios and increases thereafter, although at the 90% probability level all declines remain below 4%. Flooding of this range of depths accounts for a relatively stable proportion of the total area flooded (baseline: 64.8%; scenarios: 60.7–69.4%). Only the 90% probability level scenarios produce increases in the

extent of the deepest (>0.4 m) flooding, with declines projected for the other scenarios (no change for two 70% probability level scenarios). The area in which flooding exceeds a depth of 0.4 m increases by between 1300 m^2 (Medium) and 1525 m^2 (High) (26.9–31.6%) for the 2050s, with the corresponding range for the 2080s being 1500 m^2 (Low and Medium) to 1625 m^2 (High) (31.1–33.7%). At the other extreme, the 10% probability level scenarios project slightly larger reductions in the extent of relatively deep flooding, with declines of between 1775 m^2 (Low) and 2050 m^2 (High) (36.8–42.5%) for the 2050s and between 2000 m^2 (Low) and 2325 m^2 (High) (41.5–48.2%) for the 2080s. Mirroring the changes in shallow flooding, inundation exceeding 0.4 m accounts for a larger proportion of the total flooded area as probability level increases. For example, whilst for the baseline it accounts for 22.7% of the total flooded area, this declines to 15.9% for $2050M_{10}$. A smaller decline to 20.8% occurs for $2050M_{50}$, whilst deeper flooding accounts for 28.2% of the area inundated in $2050M_{90}$. The corresponding figures for the 2080s are 15.6, 20.5 and 29.1%, respectively.

Table 4 demonstrates that for the second event all scenarios project declines in total flood extent compared to the baseline. In common with the largest event of the simulation period, the magnitudes of the declines in inundated area are greater for the lowest probability level and decline with increasing probability. For example, the total area shown during this event for the $2050M_{10}$ scenario is 8850 m^2 (36.3%) smaller than the baseline area of 24 375 m^2. The magnitude of this decline reduces to 4675 m^2 (19.2%) for $2050M_{50}$, whilst for $2050M_{90}$ total flood extent declines by only 1425 m^2 (5.8%). This trend is repeated for the 2080s, with the corresponding reductions for the same probability levels and the Medium emission scenario being 9600, 5650 and 2575 m^2, respectively (39.4, 23.2 and 10.6%). The same pattern of declines for all the scenarios in the extent of shallow (<0.05m) flooding is displayed in Table 4. The largest declines in percentage terms are associated with the extreme (10 and 90%) probabilities, with the magnitude of the reductions declining towards the more central probabilities. For example, for 2050M the 10% probability level is associated with a decline of 4175 m^2 (38.5%). This declines to 3075 m^2 (28.3%) for 50%, only to increase to 3650 m^2 (33.6%) for the 90% probability level. The equivalent figures for 2080M are 4450 m^2 (41.0%), 3850 m^2 (35.5%) and 4925 m^2 (45.4%). Unsurprisingly, shallow flooding makes up a greater proportion of the total flood extent compared to the larger event shown in Figure 9, with a range of between

25.1 and 45.9% (mean 37.3%), a decline in all but one case ($2050L_{10}$) from the baseline (44.5%).

Despite the declines in total flood extent for all the scenarios during the 28 May 2007 event, the extent of deeper inundation does appear to increase for the two 90% probability level scenarios (Fig. 9). In particular, the width of the more deeply flooded area linked to the floodplain ditch expands. Table 4 shows that the extent of flooding of both the 0.05–0.4 m and >0.4 m depth ranges increases for this as well as the 70% probability level, following the patterns of increases in Q5 discharges and the frequency of post-restoration bankfull discharge exceedence (Table 2). For the $2050M_{90}$ and $2080M_{90}$ scenarios shown in Figure 9, the area flooded to depths above 0.4 m increases by 525 m^2 (19.6%) and 550 m^2 (20.6%), respectively, compared to the baseline (2675 m^2). At the other extreme, reductions in the extent of this relatively deep flooding are projected for the 10% probability level with, for example, declines of 900 m^2 (33.6%) and 1025 m^2 (38.3%) for the Medium emission scenario in the 2050s and 2080s, respectively. The comparable figures for the 0.05–0.4 m depth range are declines of 3775 m^2 (34.8%) and 4125 m^2 (38.0%). The central (50%) probability level scenarios project a reasonably consistent decline of between 200 m^2 (7.4%) and 275 m^2 (10.3%) in the area flooded to depths in excess of 0.4 m in both time slices. Declines of similar magnitude in percentage terms are projected for the 0.05–0.4 m depth range. The areas flooded within this range make up an almost consistently larger proportion of the total area flooded (range: 43.4–59.0%, mean: 50.0%, exceptions being the two Low, 10% probability scenarios) compared to the baseline (44.5%), whilst results for the deepest range are variable, with some declines from the baseline (11.0%) for the lowest probability level and increases for higher probabilities, although they never exceed 16.0%.

Discussion

Uncertainty in the direction of floodplain hydrological changes at Hunworth Meadow is driven by projected changes in precipitation. As noted by Jenkins et al. (2009) and Thompson (2012), UKCP09 projections of future precipitation vary in both magnitude and direction. Whilst the changes that are as likely as not to be exceeded (50% probability level) are associated with small (1.8–3.5%) declines in annual precipitation, declines and increases of roughly equal magnitude (20–30%) are projected for those probability levels that are linked to changes that are very likely and very unlikely (10 and 90% probability) to be exceeded,

respectively. For most scenarios, summers are, to varying degrees, projected to be drier and winters wetter. In contrast, there is much less uncertainty in the direction of change in PET with increases projected for all but the lowest probability level (small decreases). This dominance of precipitation in the uncertainty of future climate, and in turn hydrological impacts, reflects other studies using projections derived from alternative parameterizations of a single GCM (e.g. House et al. 2016a) or multiple GCMs (e.g. Thompson et al. 2013, 2016, 2017, Ho et al. 2016). Whilst the figures presented herein for net precipitation provide initial indications of the potential hydrological impacts of changes in climate, they represent a simplification, since actual evapotranspiration will decline below potential rates when limited by available soil moisture, a process that is simulated by both the NAM and MIKE SHE models (Thompson et al. 2009, House et al. 2016a). Notwithstanding this issue, the uncertainty in the direction of change in net precipitation (precipitation – PET) is smaller than that of precipitation due to the moderating influence of higher PET in most scenarios. Only the 90% probability level suggests wetter (higher net precipitation) conditions at an annual level. All scenarios suggest a decline from the baseline in the number of months with positive net precipitation. Given that the changes projected for the 90% probability level are very unlikely to be exceeded, a drying trend clearly dominates.

This dominance of drier conditions is confirmed by the scenario discharge time series for the River Glaven. Mean discharge declines for all of the 10–50% probability level scenarios (and half of the 70% probability level scenarios) whilst the drying trend is even less equivocal for high and low flows; declines in Q5 and Q95 are projected for all but the 90% probability level. The simple comparison of discharge and channel capacity suggests that, for the central probability level, the incidence of extensive overbank flooding will be at least halved and for the extreme low probability (10%) cut to one event in 10 years. Only the 90% (and hence very unlikely) probability level suggests increased frequency of such flooding (with an additional two events for all the scenarios of this probability level). Performance of the relatively simple lumped conceptual NAM rainfall–runoff model used in the derivation of these scenario discharges is generally very good at a monthly time step, although at smaller time steps the model underperforms in simulating some peak flows. Since this may, as suggested above, be related to landscape heterogeneity (Fiener et al. 2011), more distributed modelling approaches might improve performance. For example, in their assessment of climate change impacts,

Singh et al. (2010, 2011) employed MIKE SHE models of upstream catchments that included spatially distributed land cover to provide river flows to a wetland model. In the case of the Glaven this would require not only the distribution of different land cover types, which could be obtained from digital map data or remote sensing (e.g. Thompson 2012), but also, in order to accurately represent the agricultural landscape, details on crop types and their rotation, information that might not be readily available across the whole catchment. Given that the NAM model was used to derive monthly delta factors that were then used to perturb gauged discharges and so provide boundary conditions for the Hunworth MIKE 11 model (House et al. 2016a) rather than driving this latter model directly, its performance at a monthly time step is nonetheless considered suitable for the approach employed in this study. It is appropriate to acknowledge the inherent assumption that catchment rainfall–runoff processes, including those related to land cover, are not modified as a result of climate change. Climate change is, however, likely to lead to agricultural changes including shifts in growing seasons and crop species (e.g. Olesen and Bindi 2002, Bindi and Olesen 2011), which, given the important influence of land cover on runoff (e.g. Brown et al. 2005), creates additional uncertainty in future river flows.

Drier conditions predominate on the floodplain, with reductions in water table elevation and flood extent being projected for most scenarios. The greatest changes occur in summer when the largest reductions in water table elevation are projected, although the magnitude of these declines varies from year to year. All scenarios, irrespective of probability level, project declining mean summer water table elevations, with the result that WTE-95 declines. Away from the river (e.g. Well 1.4) these declines are at least 0.11 and 0.18 m for the 2050s and 2080s, respectively (in both cases for the L_{90} scenarios), and for the H_{10} scenarios in these same two time slices are at least 0.31 and 0.34 m, respectively. In most scenarios, the water table still reaches the surface, although the length of the period of high levels declines with probability level. Changes in peak and WTE-5 are small (e.g. no more than 0.01 m for Well 1.4), since groundwater that intercepts the surface is distributed across the floodplain, supplementing any surface inundation. The overall result of these changes is enhanced seasonality in floodplain water table elevation, echoing studies of the impacts of climate change upon UK river flows (e.g. Romanowicz et al. 2006, Johnson et al. 2009, Thompson 2012) and wetland groundwater levels (e.g. Acreman et al. 2009, Thompson et al. 2009, Herrera-Pantoja et al. 2012). Groundwater elevations closer to the river under both baseline and scenario conditions are more dynamic than across the wider floodplain, most likely due to the influence of relatively slow bi-directional sub-surface exchange between the shallow floodplain aquifer and the river (Clilverd et al. 2013) and, following embankment removal, localized inundation of the immediate riparian area and the subsequent drainage of water back to the river (Clilverd et al. 2016). However, they still, undergo the same pattern of enhanced seasonality, albeit of a smaller magnitude due to the moderating influence of their proximity to the river (e.g. declines in WTE-95 at Well 1.1 are approximately half as large as those at Well 1.4).

The impacts of a given climate change scenario upon the extent of inundation during an individual flood event will vary with a number of factors. These include the original baseline discharge, which will determine whether the perturbed scenario discharge exceeds the critical bankfull threshold, as well as the original total extent of inundation and its depth distribution. The perturbed discharge itself depends upon the date of the event, and hence the discharge delta factor, whilst the impact of an overbank event – should it occur – will be conditioned by antecedent hydrological conditions on the floodplain, such as water table elevations and soil moisture (Baker et al. 2009), which themselves will vary with time of year and scenario. The multiple factors account for the relatively large inter-event range in the reductions in total flood extent reported for any single scenario. Irrespective of these issues, declines in flood extent dominate the scenario results and, even for the highest (90%) probability level, declines in the total area of inundation are projected for at least three of the events for which baseline discharges were above bankfull capacity. Clilverd et al. (2016) argued that removal of the embankments bordering the River Glaven has promoted drainage of water from the floodplain towards the river as levels in the latter decline. Any increases in flood extent projected by individual scenarios as a result of increases in river flow or higher water tables are therefore likely to be short-lived.

Given the reported strong controls exerted by hydrological conditions upon wetland vegetation (Baldwin et al. 2001, Wheeler et al. 2009), animals (Ausden et al. 2001, McMenamin et al. 2008) and biogeochemical cycling (McClain et al. 2003, Lischeid et al. 2007), the changes reported for Hunworth Meadow will have likely implications beyond modifications to groundwater levels and flood extent. For example, wetland plant species and communities have specific and critical ecohydrological requirements that

include characteristics of the water level regime (e.g. Wheeler et al. 2004) such that even relatively small changes in the depth to the water table as well as the frequency, depth and duration of flooding could lead to shifts significant shifts in the vegetation composition (e.g. Duranel et al. 2007, Old et al. 2008). Combining the ecological requirements, if they are known, of a site's vegetation with modelled water table elevation provides a means of assessing if a specific scenario is likely to cause water tables to be "out of regime" or at risk of moving out of the regime required for specific current or target vegetation communities. Similarly, relationships between hydrological conditions (including wetland water table elevation and flood extent as well as river discharge and level) and other biota including invertebrates, fish and birds have been used to assess climate change-related implications for these species (e.g. Thompson et al. 2009, Carroll et al. 2015, House et al. 2016a, 2017). These approaches require hydrological models, such as the MIKE SHE model of Hunworth Meadow, that can accurately simulate hydrological conditions at a resolution commensurate with the magnitude of hydrological change likely to lead to ecological responses (Wheeler et al. 2004). House et al. (2016a), for example, assessed the implications of climate change-driven modifications to hydrological conditions within a riparian wetland in southeast England upon the MG8 vegetation community (Cynosurus cristatus–Caltha palustris grassland) of the UK NVC (Rodwell 1992), a community of nature conservation concern. They demonstrated a general reduction in suitability of future hydrological conditions for this community based on MIKE SHE simulated water table levels and estimates of desirable water table depths. Similarly, Thompson et al. (2009) used the sum exceedence value for aeration stress (SEVas) approach proposed by Sieben (1965), and adapted to wet grassland communities by Gowing et al. (1998), to identify potential loss of specialized wetland plants due to climate change-induced declining groundwater levels within the Elmley Marshes, an internationally important site in southeast England. This approach uses water table position as a proxy for aeration stress. A MIKE SHE model provided simulated water table elevations for climate scenarios taken from UKCIP02, the preceding generation of UK climate projections to those employed in the current study.

A preliminary analysis for Hunworth Meadow, using the same SEVas approach and simulated water table elevations for the two wells on the floodplain for which detailed results are presented above, suggests declines in mean annual SEVas, and hence soil anoxia, for all scenarios for Well 1.4 and all but 2050L$_{90}$ (+2%)

for Well 3.2. At both wells the 50% probability level is associated with declines in SEVas of around 28 and 33% in the 2050s and 2080, respectively, with limited variations between emission scenarios. For the extreme low (10% probability) the mean declines in SEVas at Well 3.2, which is on the drier part of the floodplain, are around 50 and 55% for the two time slices. The wetter conditions at Well 1.4 induce smaller changes (37 and 41%, respectively). At the other extreme (90% probability), larger SEVas reductions are projected at the latter well (2050s: 11%; 2080s: 18%) in contrast to Well 3.2 (increase of 0.3%, decrease of 5%, respectively). Given this spatial variability, linking changes in SEVas to the detailed vegetation surveys presented by Clilverd (2016) would be a useful extension of the work presented herein, and could provide a site-wide assessment of vegetation responses to hydrological changes. Additional drivers of change that would merit inclusion in such an assessment could include changes in nutrient dynamics linked to the role of floods in delivering nutrient-rich water and flood-deposited sediment, which in turn increases habitat heterogeneity (e.g. Gowing et al. 2002, Woodcock et al. 2005) and rates of biogeochemical cycling (e.g. Pinay et al. 2002). Embankment removal and the resultant increased frequency of inundation may have increased nutrient enrichment from this source with implications for plant species richness (e.g. Verhoeven et al. 1996, Michalcová et al. 2011, Clilverd et al. 2013, 2016). However, most climate change scenarios suggest a decline in the frequency and extent of inundation which would, in turn, diminish this source of nutrients, while information on sediment deposition rates and nutrient concentrations is currently lacking, leading to further uncertainties in potential future hydro-ecological conditions within Hunworth Meadow. That said, embankment removal, even under the lowest probability level scenarios, still means that at least one event during the 10-year simulation period employed in this study exceeds bankfull channel capacity, whilst the higher pre-restoration channel capacity is not exceeded by the discharge for the baseline or any of the climate change scenarios. This suggests that some benefits of embankment removal, such as increasing habitat connectivity and heterogeneity from flood disturbance by, for example, facilitating seed dispersal (Merritt et al. 2010, Nilsson et al. 2010), are likely to be retained. Floodplain restoration may, therefore, facilitate some adaptation to the predominantly drier conditions with benefits for floodplain ecological integrity that would not be possible on floodplains that remain largely isolated from the adjacent river channels.

Conclusions

The application of an existing MIKE SHE/MIKE 11 model, a new NAM rainfall–runoff model and a selection of scenarios drawn from the UKCP09 projections representing different probabilities for low, medium and high emission scenarios for the 2050s and 2080s has enabled assessments of the potential impacts of climate change, and their associated uncertainty, on hydrological conditions within the floodplain of the Hunworth Meadow restoration site in North Norfolk. There is some uncertainty in the direction of change in precipitation depending upon probability levels. Annual precipitation declines for probability levels of 50% and below, with the magnitude of declines generally increasing with declining probability, higher emission scenario and more distant time slice. The 50% probability level, associated with changes that are as likely as not to be exceeded, projects small declines (<3.5%). Direction of monthly precipitation change also varies with probability level; more central probabilities suggest wetter winters and drier summers, whilst year-round declines/increases are projected for the two extreme probability levels. In contrast, with the exception of the 10% probability level, PET increases for all scenarios, with larger changes projected for higher probability levels and emission scenarios, and the more distant time slice. To some extent, the larger gains in PET for higher probability levels counteract increases in precipitation. Only the 90% probability level scenarios suggest higher annual net precipitation, whilst all scenarios project declines in the frequency of months with positive net precipitation.

Scenario river discharge is predominantly lower than the baseline. All of the 10–50% and half of the 70% probability level scenarios experience reductions in mean discharge. For the 50% probability level, these declines are around 11–12% (2050s) and 11–17% (2080s). High and low flows, represented by Q5 and Q95 discharges, decline for all scenarios except those of the 90% probability level. The magnitude of changes in high flows, which are of particular significance given the impacts on potential inundation of the adjacent floodplain, are in percentage terms very similar to those for mean discharge. The incidence of bankfull discharges being exceeded declines for all but the 90% probability level and is at least halved for the 50% probability level.

For most climate change scenarios Hunworth Meadow becomes drier. Whilst in most cases the floodplain water table simulated by MIKE SHE still reaches the ground surface, the period of high groundwater declines with increasing probability level, emission scenario and future time slice, whilst any increases in the highest water tables are very small (<0.05m). All scenarios project a decline in summer water tables and hence enhanced seasonality in groundwater levels. Larger declines are simulated on the floodplain compared to locations closer to the river. Simulated flood extent on the Meadow declines for the vast majority of scenarios, with increases only projected for the 90% probability level. Since such changes are very unlikely to be exceeded it can be concluded that declines in flood extent will dominate. The magnitude of these declines varies from event to event but follows the general pattern of becoming more severe with lower probability level, higher emission scenario and future time slice. These hydrological changes are likely to induce ecological responses with, for example, the dominant drier conditions reducing aeration stresses to which the current vegetation has become largely adapted, potentially allowing stronger competitors to invade parts of the site. The nature of these ecological impacts may, however, also be conditioned by additional factors themselves linked to hydrological modifications such as changes in flood-borne sediment and nutrients as well as wider catchment rainfall–runoff processes.

Disclosure statement

No potential conflict of interest was reported by the authors.

References

Acreman, M.C., *et al.*, 2007. Hydrological science and wetland restoration: some case studies from Europe. *Hydrology and Earth System Sciences*, 11, 158–169. doi:10.5194/hess-11-158-2007

Acreman, M.C., *et al.*, 2009. A simple framework for evaluating regional wetland ecohydrological response to climate change with case studies from Great Britain. *Ecohydrology*, 2, 1–17. doi:10.1002/eco.v2:1

Acreman, M.C., Riddington, R., and Booker, D.J., 2003. Hydrological impacts of floodplain restoration: a case study of the River Cherwell. *Hydrology and Earth System Sciences*, 7, 75–85. doi:10.5194/hess-7-75-2003

Addy, S., *et al.*, 2016. *River restoration and biodiversity: nature-based solutions for restoring rivers in the UK and Republic of Ireland*. Aberdeen: Scotland's Centre of Expertise for Waters (CREW).

Antheunisse, A.M., *et al.*, 2006. Regional differences in nutrient limitation in floodplains of selected European rivers. *River Research and Applications*, 22, 1039–1055. doi:10.1002/rra.956

Arnell, N., 2004. Climate change impacts on river flows in Britain: the UKCIPO2 scenarios. *Water and Environment Journal*, 18, 112–117. doi:10.1111/wej.2004.18.issue-2

Arnell, N. and Reynard, N., 1996. The effects of climate change due to global warming on river flows in Great Britain. *Journal of Hydrology*, 183, 397–424. doi:10.1016/0022-1694(95)02950-8

Arthington, A.H., *et al.*, 2015. Biodiversity values of remnant freshwater floodplain lagoons in agricultural catchments: evidence for fish of the Wet Tropics bioregion, northern Australia. *Aquatic Conservation: Marine And Freshwater Ecosystems*, 25, 336–352. doi:10.1002/aqc.v25.3

Ausden, M., Sutherland, W.J., and James, R., 2001. The effects of flooding lowland wet grassland on soil macroinvertebrate prey of breeding wading birds. *Journal of Applied Ecology*, 38, 320–338. doi:10.1046/j.1365-2664.2001.00600.x

Baker, C., Thompson, J.R., and Simpson, M., 2009. Hydrological dynamics I: surface waters, flood and sediment dynamics. In: E.B. Maltby and T. Barker, eds. *The wetlands handbook*. Chichester: Wiley-Blackwells, 120–168.

Baker, M.A. and Vervier, P., 2004. Hydrologic variability organic matter supply and denitrification in the Garonne River ecosystem. *Freshwater Biology*, 49, 181–190. doi:10.1046/j.1365-2426.2003.01175.x

Baldwin, A., Egnotovich, M., and Clarke, E., 2001. Hydrologic change and vegetation of tidal freshwater marshes: field, greenhouse, and seed-bank experiments. *Wetlands*, 21, 519–531. doi:10.1672/0277-5212(2001)021[0519:HCAVOT]2.0.CO;2

Bates, B.C., *et al.*, eds., 2008. *Climate change and water. Technical paper of the intergovernmental panel on climate change*. Geneva: IPCC Secretariat.

Bernhardt, E.S., *et al.*, 2005. Synthesizing U.S. river restoration efforts. *Science*, 308, 636–637. doi:10.1126/science.1109769

Bindi, M. and Olesen, J.E., 2011. The responses of agriculture in Europe to climate change. *Regional Environmental Change*, 11 (Supplement 1), 151–158. doi:10.1007/s10113-010-0173-x

Blackwell, M. and Maltby, E., eds., 2006. *Ecoflood Guidelines How to use floodplains for flood risk reduction*. Brussels: European Commission.

Brown, A.E., *et al.*, 2005. A review of paired catchment studies for determining changes in water yield resulting from alterations in vegetation. *Journal of Hydrology*, 310, 28–61. doi:10.1016/j.jhydrol.2004.12.010

Buijse, A.D., *et al.*, 2002. Restoration strategies for river floodplains along large lowland rivers in Europe. *Freshwater Biology*, 47, 889–907.

Bullock, A. and Acreman, M.C., 2003. The role of wetlands in the hydrological cycle. *Hydrology and Earth System Sciences*, 7, 75–86.

Canadell, J., *et al.*, 1996. Maximum rooting depth for vegetation types at the global scale. *Oecologia*, 108, 583–595.

Carroll, M.J., *et al.*, 2015. Hydrologically driven ecosystem processes determine the distribution and persistence of ecosystem-specialist predators under climate change. *Nature Communications*, 6, 7851. doi:10.1038/ncomms8851

Castellarin, A., Di Baldassarre, G., and Brath, A., 2010. Floodplain management strategies for flood attenuation in the river Po. *River Research and Applications*, 27, 1037–1047.

Chiew, F., *et al.*, 1995. Simulation of the impacts of climate change on runoff and soil moisture in Australian catchments. *Journal of Hydrology*, 167, 121–147.

Chubarova, N.P., 1972. Computation of the height of capillary rise of water in different genetic types of bound soils. *Soil Mechanics and Foundation Engineering*, 9, 25–27.

Clilverd, H.M., *et al.*, 2013. River-floodplain hydrology of an embanked lowland Chalk river and initial response to embankment removal. *Hydrological Sciences Journal*, 58, 627–650.

Clilverd, H.M., *et al.*, 2016. Coupled hydrological/hydraulic modelling of river restoration impacts and floodplain hydrodynamics. *River Research and Applications*, 32, 1927–1948.

Clilverd, H.M., 2016. *Hydroecological monitoring and modelling of river-floodplain restoration in a UK lowland river meadow*. PhD thesis. UCL, London.

Clilverd, H.M., 2016. Simulated effects of river restoration on soil aeration status and plant community composition. doi/10.1002/rra.3036/pdf

Darby, S. and Sear, D., eds., 2008. *River restoration: managing the uncertainty in restoring physical habitat*. Chichester: Wiley.

Das, B.M., 2002. *Principles of geotechnical engineering*. 5th ed. Pacific Grove, CA: Brooks/Cole.

DHI, 2007. *MIKE SHE user manual*. Hørsholm, Denmark: DHI – Water & Environment.

DHI, 2009. *MIKE 11 a modelling system for rivers and channels: reference manual*. Hørsholm: DHI Water and Environment.

Duranel, A., *et al.*, 2016. Integrated hydrological modelling of a groundwater-dependent valley mire in central France. In: *Groundwater: managing our Hidden Asset*, 13–14 September 2016. Birmingham, UK. Available from: http://www.iah-british.org/wp-content/uploads/2016/07/Hydrogeology_of_Peat_July2016_Abstracts.pdf

Duranel, A.J., *et al.*, 2007. Assessing hydrological suitability of the Thames floodplain for species-rich meadow restoration. *Hydrology and Earth System Sciences*, 11, 170–179.

Dwire, K.A., Boone Kauffman, J., and Baham, J.E., 2006. Plant species distribution in relation to water-table depth

and soil redox potential in montane riparian meadows. *Wetlands*, 26, 131–146.

Environment Agency, 2010. *River habitats in England and Wales: current state and changes since 1995–96*. Bristol: Environment Agency.

Erskine, W.D., 1992. Channel response to large-scale river training works: hunter river, Australia. *Regulated Rivers: Research and Management*, 7, 261–278.

Erwin, K.L., 2009. Wetlands and global climate change: the role of wetland restoration in a changing world. *Wetlands Ecology and Management*, 17, 71–84.

FAO, 2013. *Crop Water Information: Wheat (WWW)*. Rome, Italy, Food and Agriculture Organization of the United Nations (FAO) Water and Development Unit. Available from: wwwfaoorg/nr/water/cropinfo_wheathtml [Accessed 21 September 2013].

Fiener, P., Auerswald, K., and Van Oost, K., 2011. Spatio-temporal patterns in land use and management affecting surface runoff response of agricultural catchments—A review. *Earth-Science Reviews*, 106, 92–104.

Flynn, N.J., *et al.*, 2002. Macrophyte and periphyton dynamics in a UK Cretaceous Chalk stream: the River Kennet, a tributary of the Thames. *Science of the Total Environment*, 23, 282–283.

Forshay, K.J. and Stanley, E., 2005. Rapid nitrate loss and denitrification in a temperate river floodplain. *Biogeochemistry*, 75, 43–64.

Freeman, M.C., Pringle, C.M., and Jackson, C.R., 2007. Hydrologic connectivity and the contribution of stream headwaters to ecological integrity at regional scales. *Journal of the American Water Resources Association*, 43, 5–14.

Gowing, D.G., Spoor, G., and Mountford, O., 1998. The influence of minor variations in hydrological regime on grassland plant communities: implications for water management. In: C.B. Joyce and P.M. Wade, eds. *European wet grasslands: biodiversity, management and restoration*. Chichester: Wiley, 217–227.

Gowing, D.J.G., *et al.* 2002. *A review of the ecology, hydrology and nutrient dynamics of floodplain meadows in England*. Peterborough: English Nature, English Nature Research Reports - No. 446.

Graham, L.P., *et al.*, 2007. On interpreting hydrological change from regional climate models. *Climatic Change*, 81, 97–122.

Grevilliot, F., Krebs, L., and Muller, S., 1998. Comparative importance and interference of hydrological conditions and soil nutrient gradients in floristic biodiversity in flood meadows. *Biodiversity and Conservation*, 7, 1495–1520.

Hafezparast, M., Araghinejad, S., and Fatemi, S.E., 2013. A conceptual rainfall-runoff model using the auto calibrated NAM models in the Sarisoo River. *Hydrology Current Research*, 4, 148. doi:10.4172/2157-7587.1000148

Hammersmark, C.T., Cable Rains, M., and Mount, J.F., 2008. Quantifying the hydrological effects of stream restoration in a montane meadow Northern California USA. *River Research and Applications*, 24, 735–753.

Henriksen, H.J., *et al.*, 2003. Methodology for construction, calibration and validation of a national hydrological model for Denmark. *Journal of Hydrology*, 280, 52–71.

Henriksen, H.J., *et al.*, 2008. Assessment of exploitable groundwater resources of Denmark by use of ensemble resource indicators and a numerical groundwater–surface water model. *Journal of Hydrology*, 348, 224–240.

Herbst, M., *et al.*, 2008. Comparative measurements of transpiration and canopy conductance in two mixed deciduous woodlands differing in structure and species composition. *Tree Physiology*, 28, 959–970.

Herrera-Pantoja, M., Hiscock, K., and Boar, R., 2012. The potential impact of climate change on groundwater-fed wetlands in eastern England. *Ecohydrology*, 5, 401–413.

Hill, A.R., 1996. Nitrate removal in stream riparian zones. *Journal of Environmental Quality*, 25, 743–755.

Ho, J.T., Thompson, J.R., and Brierley, C.B., 2016. Projections of hydrology in the Tocantins-Araguaia Basin, Brazil: uncertainty assessment using the CMIP5 ensemble. *Hydrological Sciences Journal*, 61, 551–567.

Hough, M.N. and Jones, R.J.A., 1997. The United Kingdom Meteorological Office Rainfall and Evaporation Calculation System: MORECS version 2.0 – an overview. *Hydrology and Earth System Sciences*, 1, 227–239.

House, A.R., *et al.*, 2016b. Modelling groundwater/surface-water interaction in a managed riparian chalk valley wetland. *Hydrological Processes*, 30, 447–462.

House, A.R., *et al.*, 2017. Projecting impacts of climate change on habitat availability in a macrophyte dominated chalk river. *Ecohydrology*. doi:10.1002/eco.1823

House, A.R., Thompson, J.R., and Acreman, M.C., 2016a. Projecting impacts of climate change on hydrological conditions and biotic responses in a chalk valley riparian wetland. *Journal of Hydrology*, 534, 178–192.

IPCC, 2000. *Special Report on Emissions Scenarios (SRES): A special report of Working Group III of the Intergovernmental Panel on Climate Change*. Cambridge: Cambridge University Press.

IPCC, 2014. *Climate change 2014: synthesis report. Contribution of Working Groups I, II and III to the Fifth Assessment Report of the Intergovernmental Panel on Climate Change*. Geneva: IPCC.

Jenkins, G.J., *et al.*, 2009. *UK Climate Projections: briefing Report*. Exeter: Met Office Hadley Centre.

Johnson, A.C., *et al.*, 2009. The British river of the future: how climate change and human activity might affect two contrasting river ecosystems in England. *Science of the Total Environment*, 407, 4787–4798.

Junk, W.J., Bayley, P.B., and Sparks, R.E., 1989. The flood pulse concept in river floodplain systems. In: D.P. Doge, ed. *Proceedings of the International Large River Symposium*. Ottawa: Canadian Special Publication of Fisheries and Aquatic Sciences, Vol. 106, 110–127.

Karim, F., *et al.*, 2016. Impact of climate change on floodplain inundation and hydrological connectivity between wetlands and rivers in a tropical river catchment. *Hydrological Processes*, 30, 1574–1593.

Kondolf, G.M., 1995. Five elements for effective evaluation of stream restoration. *Restoration Ecology*, 3, 133–136.

Kondolf, G.M., *et al.*, 2006. Process-based ecological river restoration: visualizing three-dimensional connectivity and dynamic vectors to recover lost linkages. *Ecology and Society*, 11 (2), 5. Available from: http://www.ecologyandsociety.org/vol11/iss2/art5/

Kundzewicz, Z.W., et al., 2007. Freshwater resources and their management. In: M.L. Parry, et al., eds. Climate change 2007: impacts, adaptation and vulnerability. Contribution of Working Group II to the Fourth Assessment Report of the Intergovernmental Panel on Climate Change. Cambridge: Cambridge University Press, 173–210.

Lischeid, G., et al., 2007. Impact of redox and transport processes in a riparian wetland on stream water quality in the Fichtelgebirge region, southern Germany. Hydrological Processes, 21, 123–132.

Madsen, H., 2000. Automatic calibration of a conceptual rainfall-runoff model using multiple objectives. Journal of Hydrology, 235, 276–288.

Madsen, H., 2003. Parameter estimation in distributed hydrological catchment modelling using automatic calibration with multiple objectives. Advances in Water Resources, 26, 205–216.

McClain, M.E., et al., 2003. Biogeochemical hot spots and hot moments at the interface of terrestrial and aquatic ecosystems. Ecosystems, 6, 301–312.

McMenamin, S.K., Hadly, E.A., and Wright, C.K., 2008. Climatic change and wetland desiccation cause amphibian decline in Yellowstone National Park. Proceedings of the National Academy of Sciences, 105, 16988–16993.

Merritt, D.M., Nilsson, C., and Jansson, R., 2010. Consequences of propagule dispersal and river fragmentation for riparian plant community diversity and turnover. Ecological Monographs, 80, 609–626.

Michalcová, D., et al., 2011. The combined effect of waterlogging, extractable P and soil pH on α-diversity: a case study on mesotrophic grasslands in the UK. Plant Ecology, 212, 879–888.

Monteith, J.L., 1965. Evaporation and the environment. Symposia of the Society for Experimental Biology, 19, 205–234.

Moorlock, B.S.P., et al. 2002. Geology of the Cromer District – a brief explanation of the geological map, Sheet Explanations of the British Geological Survey. 1:50000 Sheet 131 Cromer (England and Wales). Nottingham, UK: BGS.

Muhar, S., Schmutz, S., and Jungwirth, M., 1995. River restoration concepts - goals and perspectives. Hydrobiologia, 303, 183–194.

Murphy, J.M., et al., 2009. UK Climate Projections Science Report: climate change projections. Exeter: Met Office Hadley Centre.

Naiman, R.J., Decamps, H., and McClain, M.E., 2010. Riparia: ecology conservation and management of streamside communities. London: Elsevier Academic Press.

Nash, I.E. and Sutcliffe, I.V., 1970. River flow forecasting through conceptual models. Journal of Hydrology, 10, 282–290.

Nilsson, C., et al., 2010. The role of hydrochory in structuring riparian and wetland vegetation. Biological Reviews, 85, 837–858.

Nilsson, C. and Svedmark, M., 2002. Basic principles and ecological consequences of changing water regimes: riparian plant communities. Environmental Management, 30, 468–480.

Old, G., et al. 2008. Methods to assess, model and map the environmental consequences of flooding - Literature review. Bristol: Environment Agency, Environment Agency Science Report SC060062.

Olesen, J.E. and Bindi, M., 2002. Consequences of climate change for European agricultural productivity, land use and policy. European Journal of Agronomy, 16, 239–262.

Pedroli, B., et al., 2002. Setting targets in strategies for river restoration. Landscape Ecology, 17, 5–18.

Pescott, O. and Wentworth, J., 2011. Postnote: natural flood management. London: Houses of Parliament Parliamentary Office of Science and Technology.

Petts, G. and Calow, P., eds., 1996. River restoration. Selected extracts from "The Rivers Handbook". Oxford: Blackwell Science.

Pinay, G., Clément, J.C., and Naiman, R.J., 2002. Basic principles and ecological consequences of changing water regimes on nitrogen cycling in fluvial systems. Environmental Management, 30, 481–491.

Rodwell, J.S., 1992. British plant communities. Volume 3 - Grasslands and montane communities. Cambridge: CUP.

Romanowicz, R., et al., 2006. Effects of climate change on river flows and groundwater recharge, a practical methodology. London: UKWIR, Interim report on Rainfall-Runoff Modelling, UKWIR report CL/04.

Sieben, W.H., 1965. Het verband tussen outwatering en opbrengst bij de jonge zavelgronden in de Noordoostpolder. Van Zee Tot Land, 40, 1–117.

Silvertown, J., et al., 1999. Hydrologically defined niches reveal a basis for species richness in plant communities. Nature, 400, 61–63.

Singh, C.R., et al., 2010. Modelling the impact of prescribed global warming on runoff from headwater catchments of the Irrawaddy River and their implications for the water level regime of Loktak Lake, northeast India. Hydrology and Earth System Sciences, 14, 1745–1765.

Singh, C.R., et al., 2011. Modelling water-level options for ecosystem services and assessment of climate change: loktak Lake, northeast India. Hydrological Sciences Journal, 56, 1518–1542.

Thompson, J.R., et al., 2004. Application of the coupled MIKE SHE/MIKE 11 modelling system to a lowland wet grassland in Southeast England. Journal of Hydrology, 293, 151–179.

Thompson, J.R., 2004. Simulation of wetland water level manipulation using coupled hydrological/hydraulic modelling. Physical Geography, 25, 39–67.

Thompson, J.R., et al., 2009. Modelling the hydrological impacts of climate change on UK lowland wet grassland. Wetlands Ecology and Management, 17, 503–523.

Thompson, J.R., 2012. Modelling the impacts of climate change on upland catchments in southwest Scotland using MIKE SHE and the UKCP09 probabilistic projections. Hydrology Research, 43, 507–530.

Thompson, J.R., et al., 2013. Assessment of uncertainty in river flow projections for the Mekong River using multiple GCMs and hydrological models. Journal of Hydrology, 486, 1–30.

Thompson, J.R., Crawley, A., and Kingston, D.G., 2016. GCM-related uncertainty for river flows and inundation under climate change: the Inner Niger Delta. Hydrological Sciences Journal, 61, 2325–2347.

Thompson, J.R., Crawley, A., and Kingston, D.G., 2017. Future river flows and flood extent in the Upper Niger and Inner Niger Delta: GCM-related uncertainty using the CMIP5 ensemble. Hydrological Sciences Journal, 62. doi:10.1080/02626667.2017.1383608

Thompson, J.R., Green, A.J., and Kingston, D.G., 2014. Potential evapotranspiration-related uncertainty in climate change impacts on river flow: an assessment for the Mekong River basin. *Journal of Hydrology*, 510, 259–279.

Thorup-Kristensen, K., Salmerón Cortasa, M., and Loges, R., 2009. Winter wheat roots grow twice as deep as spring wheat roots is this important for N uptake and N leaching losses? *Plant and Soil*, 322, 101–114.

Tockner, K., et al., 1999. Hydrological connectivity, and the exchange of organic matter and nutrients in a dynamic river–floodplain system (Danube, Austria). *Freshwater Biology*, 41, 521–535.

Tockner, K. and Stanford, J.A., 2002. Riverine flood plains: present state and future trends. *Environmental Conservation*, 29, 308–330.

USDA, 1986. *Urban hydrology for small watersheds*. Washington, DC: USDA. Technical Release 55 (TR-55).

Verhoeven, J.T.A., Koerselman, W., and Meuleman, A.F.M., 1996. Nitrogen- or phosphorus-limited growth in herbaceous, wet vegetation: relations with atmospheric inputs and management regimes. *Trends in Ecology & Evolution*, 11, 494–497.

Viers, J.H., et al., 2012. Multiscale patterns of riparian plant diversity and implications for restoration. *Restoration. Ecology*, 20, 160–169.

Ward, J.V., 1998. Riverine landscapes: biodiversity patterns, disturbance regimes, and aquatic conservation. *Biological Conservation*, 83, 269–278.

Ward, J.V., et al., 2002. Riverine landscape diversity. *Freshwater Biology*, 47, 517–539.

Ward, J.V. and Stanford, J.A., 1995. Ecological connectivity in alluvial river ecosystems and its disruption by flow regulation. *Regulated Rivers: Research and Management*, 11, 105–119.

Ward, J.V., Tockner, K., and Schiemer, F., 1999. Biodiversity of floodplain river ecosystems: ecotones and connectivity. *Regulated Rivers: Research and Management*, 15, 125–139.

Wheeler, B., Shaw, S., and Tanner, K. 2009. *A wetland framework for impact assessment at statutory sites in England and Wales*. Bristol: Environment Agency, Environment Agency Science Report SC030232.

Wheeler, B.D., et al., 2004. *Ecohydrological guidelines for lowland plant communities*. Peterborough: Environment Agency (Anglian) Region.

Woodcock, B.A., et al., 2005. Re-creation of a lowland flood-plain meadow: management implications for invertebrate communities. *Journal of Insect Conservation*, 9, 207–218.

Wyżga, B., 2001. Impact of the channelization-induced incision of the Skawa and Wisłoka Rivers, southern Poland, on the conditions of overbank deposition. *Regulated Rivers: Research & Management*, 17, 85–100.

Zedler, J.B. and Kercher, S., 2005. Wetland resources: status trends ecosystem services and restorability. *Annual Review of Environment and Resources*, 30, 39–74.

Zotarelli, L., Dukes, M.D., and Morgan, K.T., 2010. *Interpretation of soil moisture content to determine soil field capacity and avoid over-irrigating sandy soils using soil moisture sensors*. Gainesville, FL: WWW. http://edis.ifas.ufl.edu/ae460 [Accessed 26 September 2012].